We put science to work.™

Savannah River National Laboratory™

OPERATED BY SAVANNAH RIVER NUCLEAR SOLUTIONS

A U.S. DEPARTMENT OF ENERGY NATIONAL LABORATORY • SAVANNAH RIVER SITE • AIKEN, SC

X-ray Diffraction of Slag-based Sodium Salt Waste Forms

C.A. Langton

D.M. Missimer

September 2014

SRNL-STI-2014-00397, Revision 1

SRNL.DOE.GOV

DISCLAIMER

Printed in the United States of America

Prepared for
U.S. Department of Energy

SRNL-STI-2014-00397
Revision 1

Keywords: *Waste form characterization*

Retention: *Permanent*

X-ray Diffraction of Slag-based Sodium Salt Waste Forms

C.A. Langton
D. M. Missner

September 2014

Prepared for the U.S. Department of Energy under contract number DE-AC09-08SR22470.

Savannah River National Laboratory™
OPERATED BY SAVANNAH RIVER NUCLEAR SOLUTIONS

EXECUTIVE SUMMARY

The attached report documents sample preparation and x-ray diffraction results for a series of cement and blended cement matrices prepared with either water or a 4.4 M Na salt solution. The objective of the study was to provide initial phase characterization for the Cementitious Barriers Partnership reference case cementitious salt waste form. This information can be used to: 1) generate a base line for the evolution of the waste form as a function of time and conditions, 2) potentially to design new binders based on mineralogy of the binder, 3) understand and predict anion and cation leaching behavior of contaminants of concern, and 4) predict performance of the waste forms for which phase solubility and thermodynamic data are available.

Both water and a 4.4 M sodium salt solution were used to hydrate the cementitious reagents. One of the mixes containing the sodium salt solution and blended binder was approximated by the Cementitious Barriers reference case salt waste form. The other mixes contained combinations of the reference case binder ingredients. Mixes prepared with water were compared to literature data of typical blended cement matrices.

The intent was to use this characterization data as a starting point for more detailed phase characterization using various techniques including neutron diffraction techniques in addition to quasi-elastic neutron scattering techniques for characterization of water at the ORNL Spallation Neutron Source, Oak Ridge, TN and other methods such as, thermogravimetric techniques, electron diffraction, scanning electron microscopy and energy-dispersive X-ray spectroscopy. The initial characterization is complete. Due to extensive substitutions of cations and anions in the layered double hydroxide phases and the very fine intermixing of poorly crystalline hydrated phases in the reference case blend (10 : 45 : 45 cement : slag : fly ash), electron diffraction and transmission electron spectroscopy are recommended as the next step for characterization.

Characterization of the mineralogy and differences in the mineralogy between blended portland cement construction materials and sodium salt waste forms is also important for understanding and predicting the buffering effects that the waste form has on infiltrating water / leachates. The mineralogy of the cured cementitious matrices influences the physical properties (strength, stiffness, etc.) of the cured material due to the degree of polymerization (chain length) and tetrahedron arrangement. Information about the mineralogy of hydrated cementitious materials and blends of these ingredients is needed to design waste form matrices, select ingredients and make adjustments in material proportions. Information presented in this report is an initial step in developing phase diagrams for the hydrated systems in which caustic sodium salt solutions are used as the hydration fluid for waste forms, such as, the SRS saltstone waste form and the Hanford Cast Stone waste form.

TABLE OF CONTENTS

Executive Summary…….v

Attachment 1. X-ray Diffraction of Slag-Based Sodium Salt Waste Forms……..A-1

X-ray Diffraction of Slag-based Sodium Salt Waste Forms

Cementitious Barriers Partnership

September 2014

CBP-TR-2014-005, Rev. 1

ACKNOWLEDGEMENTS

This report was prepared for the United States Department of Energy under Interagency Agreement No. DE-AI09-09SR22667 and is an account of work performed under that contract. This report was also prepared with the financial support by the U. S. Department of Energy, under Cooperative Agreement Number DE-FC01-06EW07053 entitled 'The Consortium for Risk Evaluation with Stakeholder Participation III' awarded to Vanderbilt University. Reference herein to any specific commercial product, process, or service by trademark, name, manufacturer, or otherwise does not necessarily constitute or imply endorsement, recommendation, or favoring of same by Savannah River Nuclear Solutions, Vanderbilt University or by the United States Government or any agency thereof. The views and opinions of the authors expressed herein do not necessarily state or reflect those of the United States Government or any agency thereof. This report is part of a larger multi-investigator project supported by the U. S. Department of Energy entitled the Cementitious Barriers Partnership. The opinions, findings, conclusions, or recommendations expressed herein are those of the authors and do not necessarily represent the views of the U.S. Department of Energy. This work was also partially supported by the National Institute of Standards and Technology Sustainable, High Performance Infrastructure Materials program.

Printed in the United States of America
United States Department of Energy
Office of Environmental Management
Washington, DC

This document is available on the U.S. DOE Information Bridge and on the CBP website: http://cementbarriers.org/
An electronic copy of this document is also available through links on the following

SUMMARY

Cementitious materials are used to solidify and stabilize aqueous based radioactive waste containing sodium salts. The types and proportions of cementitious ingredients used to treat these alkaline aqueous radioactive salt waste streams depend on the performance objectives for the waste forms and the compositions of the waste streams. Matrix phases can stabilize certain contaminants by co-precipitation, substitution, exchange, and / or sorption. Matrix phases also effect processing properties and are responsible for the physical properties and durability of the cured waste forms. Consequently, characterization of the matrix (binder) mineralogy (chemical compositions and crystal structures) is important for predicting contaminant leaching and evolution of the materials as a function of time and changing conditions.

This report documents sample preparation and x-ray diffraction results for a series of materials made with water or highly alkaline sodium salt simulated waste water and cementitious binders. The objective of this study was to provide initial phase characterization for the CBP reference case cementitious salt waste form. This information can be used to: 1) generate a base line for the evolution of the waste form as a function of time and conditions, 2) potentially to design new binders based on mineralogy of the binder, 3) understand and predict anion and cation leaching behavior of contaminants of concern, and 4) predict performance of the waste forms for which phase solubility and thermodynamic data are available. Characterization of the mineralogy is also important for understanding the buffering effects that the waste form has on infiltrating water / leachates.

Identification of hydrated phases capable of sequestering anions in the structures and crystallinity of the calcium silicate binder phases were of particular interest. The intent was to use this characterization data as a starting point for more detailed phase characterization using electron and neutron diffraction techniques in addition to quasi-elastic neutron scattering techniques for characterization of water in the matrix. The initial characterization is complete.

In summary, the hydrated mixtures of Type II portland cement, Grade 100 ground granulated blast furnace slag (GGBFS) and carbon burn-out (CBO) Class F fly ash contained hydrated phase assemblages which were typical of those reported in the literature. The mineralogy and bulk oxide composition of the blends analyzed in this study controlled the mineralogy of the hydrated material. The calcium silicate hydrate phase assemblage in samples hydrated with the alkaline 4.4 M sodium salt simulated waste solution was found to be a function of the $(CaO + MgO) / (SiO_2 + Al_2O_3)$ ratio of the samples characterized. Based on x-ray diffraction results, no significant differences were detected in samples cured 2 months and 14 months in sealed containers at ambient indoor temperatures.

Slag and a blend of slag and cement hydrated with caustic 4.4 M Na salt solution resulted in the most crystalline matrix. In addition to poorly ordered C-S-H, these samples contained fairly well ordered C-S-H I (a precursor of 14Å tobermorite) and 11 Å Al-substituted tobermorite. These crystalline C-S-H phases did not form or were present in only trace amounts in slag blends containing about 45 to 62 mass percent fly ash. These slag-Class F fly ash blends had a higher silica plus alumina content relative to lime and magnesia than the blends that produced C-S-H I and Al-substituted tobermorite. The calcium silicate binder in the 10:45:45 mixture of cement : slag : fly ash was made up of poorly ordered C-S-H. The sample cured for 14 months may contain a small amount of the more crystalline calcium silicate hydrate phases.

Layered double hydroxides in the hydrotalcite (magnesium-aluminum carbonate hydroxide) and hydrocalumite / AFm phases (calcium aluminum hydroxide) were present in mixtures containing slag.

The specific phase(s) were not identified because these phases form solid solutions and have a considerable amount of overlap in their x-ray patterns.

Sodium nitrate was the only sodium salt phase identified in x-ray diffraction patterns of the samples hydrated with salt solution. Drying during x-ray diffraction sample preparation may have resulted in precipitation of the sodium nitrate or it may have been present in the samples prior to x-ray sample preparation.

Sodium sulfate, aluminate, and carbonate may have been incorporated in the structures of the layered double hydroxide (AFm) type phases. These mixed metal layered double hydroxides make up an important fraction of the matrix in the slag containing blends hydrated with caustic salt solution. They are among the few oxide-based phases that exhibit substantial, permanent anion exchange capacity [Kirkpatrick, et al. 1999, Plamer, et al., 2009, and Zhang and Reardon, 2003]. They also contribute to the structural properties of cementitious matrices [Taylor, 1997].

The mineralogy of the hydrated calcium-silicate matrices in cured cementitious waste forms influences the physical properties (strength, stiffness, porosity, hydraulic conductivity, shrinkage, expansion, etc.) of the cured waste form matrix material due to the degree of polymerization (chain length) and tetrahedron arrangement. Information about the mineralogy of hydrated cementitious materials and blends is needed to design waste forms, i.e., select ingredients and proportions. Information presented in this report is an initial step in developing phase diagrams for the hydrated systems in which caustic sodium salt solutions are used as the hydration fluid for waste forms.

ABBREVIATIONS

AAS	**Alkali Activated Slag**
ASTM	**American Society of Testing and Materials**
C-S-A-H	**Alumina Substituted Hydrated Calcium Silicate Gel (non to poorly crystalline solid)**
C-S-H	**Hydrated Calcium Silicate Gel (non to poorly ordered solid)**
DOE	**US Department of Energy**
EDX	**Energy Dispersive X-Ray**
GGBFS	**Ground Granulated Blast Furnace Slag**
ICDD	**International Center for Diffraction Data**
LDH	**Layered Double Hydroxide**
M	**Molar**
MAS	**Magic Angle Scattering**
NMR	**Nuclear Magnetic Resonance**
ORNL	**Oak Ridge National Laboratory**
R&D	**Research and Development**
rpm	**Revolutions per minute**
SEM	**Scanning Electron Microscopy**
SRNL	**Savannah River National Laboratory**
TDS	**Total Dissolved Solids**
TT/QAP	**Task Technical and Quality Assurance Plan**

TABLE OF CONTENTS

SUMMARY…….....ii

ABBREVIATIONS ……...iv

LIST OF TABLES …….……...vi

INTRODUCTION ……..…….……...1

OBJECTIVE ….…….…….……....1

BACKGROUND…..……....1

EXPERIMENTAL METHOD.……..……...……..1

LITERATURE REVIEW.……...…….…….....3

Portland Cement..…….……4

Hydrated Portland Cement …….……..….4

Ground Granulated Blast Furnace Slag ……..5

Alkali Activated Slag ……..…….….5

Class F Fly Ash …….…….……...6

Hydrated Class F Fly Ash……...…….……6

RESULTS ……...9

Anhydrous Starting Materials ……9

Hydration of Starting Materials in Water ……....9

Hydration of Starting Materials in 4.4 M Na Salt Solution……..…….……..11

Hydration of Starting Material Blends in 4.4 M Na Salt Solution..…….…….....11

DISCUSSION……14

CONCLUSIONS ….……16

REFERENCES…….…..…..17

ATTACHMENT 1. X-RAY DIFFRACTION POWDER PATTERNS….……19

ATTACHMENT 2. ANALYSIS OF INGREDIENTS USED TO PREPARE SAMPLES……..30

LIST OF TABLES

Table 1. Sodium salt waste solution with a molar composition of a simple simulated sodium salt solution. 2

Table 2. Ingredients used to prepare the simulated salt solution. 2

Table 3. Material prepared for x-ray-diffraction characterization. 3

Table 4. Portland cement mineralogy. 4

Table 5. Hydrated Portland cement mineralogy (w/c = 0.4 to 0.6; ambient temperature curing). 5

Table 6. Hydrated Slag Mineralogy. 6

Table 7. Class F fly ash mineralogy. 8

Table 8. Phases identified in XRD powder patterns of anhydrous cementitious reagents and individual hydrated materials and the corresponding International Center for Diffraction Data (ICDD) database card numbers. 10

Table 9. Phases identified in XRD powder patterns of individual cementitious materials hydrated with 4.4 M Na salt solution and the International Center for Diffraction Data (ICDD) Database Card Numbers. 12

Table 10. Phases identified in XRD powder patterns of blends of cementitious materials hydrated with 4.4 M Na salt solution and the International Center for Diffraction Data (ICDD) Database Card Numbers. 13

Table 11. Major oxide results for cement, slag and Class F fly ash. 15

Table 12. Normalized selected oxides for starting materials and four blends. 15

LIST OF FIGURES

Figure 1. Calcium silicate hydrate phases in binders hydrated with 4.4 M Na salt solution as a function of (CaO + MgO) / (Al_2O_3 + SIO_2) ratio. 16

INTRODUCTION

Cementitious materials are used to solidify and stabilize aqueous based radioactive waste containing sodium salts. The types and proportions of cementitious ingredients used to treat aqueous radioactive waste streams containing sodium salts depend on the performance objectives for the waste forms and the compositions of the waste streams. Matrix phases can stabilize certain contaminants (co-precipitation, substitution, ion exchange, and / or sorption), influence processing properties, and are responsible for physical properties and durability of the cured waste forms. Consequently, characterization of the matrix (binder) mineralogy (chemical compositions and crystalline / non crystalline structures) is important for predicting contaminant leaching and evolution of the materials as a function of time and changing conditions.

This report documents sample preparation and x-ray diffraction results for a series of mixtures of sodium salt waste and cementitious binders.

OBJECTIVE

The objective of this report was to characterize the phase assemblages in the Cementitious Barriers Partnership reference case sodium salt waste form [Langton, 2009]. This information can be used to: 1) generate a base line for the evolution of the waste form as a function of time and conditions, 2) design new binders based on matrix mineralogy, 3) understand and predict anion and cation leaching behavior of contaminants of concern, and 4) predict performance of the waste forms and 5) identify appropriate phase solubility and thermodynamic data. Characterization of the mineralogy is also important for understanding the buffering effects that the waste form has on infiltrating water / leachates.

BACKGROUND

Sodium salt waste forms generated in the DOE complex typically consist of a blend of ground granulated blast furnace slag (GGBFS), portland cement, and Class F fly ash. Blends of these ingredients have been used to treat caustic aqueous sodium salt waste streams generated from separation and recovery of isotopes for defense programs. The objective of the treatment is to provide a diffusion barrier for soluble contaminants, stabilize selected contaminants, and convert a liquid waste into a solid waste form suitable for disposal.

This effort was intended to obtain preliminary phase / mineralogy data for subsequent electron and neutron diffraction and microscopy analyses of the hydrated binder phases. An experimental plan to characterize the matrix phases was developed by SRNL researchers in conjunction E. Pierce, ORNL and documented in Task Technical and Quality Assurance Plan (TT/QAP) [Langton, 2012].

At the present time, the matrices of these cementitous waste forms are not well characterized because a large portion of the matrix is made up of phases that have poorly ordered structures and form solid solutions involving cation and anion substitutions. In addition, the matrix consists of micrometer and sub-micrometer particles inter grown to the extent that individual particles are difficult to characterize using scanning electron microscopy (SEM) and energy dispersive x-ray spectroscopy (EDX).

EXPERIMENTAL METHOD

ASTM Type I water and a simulated sodium salt waste solution were used as the mixing fluids for the materials analyzed in this study. The simulated waste solution was based on the CBP reference case salt waste form. The simple salt solution composition is provided in Tables 1 and 2. This solution had a density of 1.207 g / ml and contained 25.13 weight percent total dissolved solids (TDS).

Table 1. Sodium salt waste solution with a molar composition of a simple simulated sodium salt solution.

Component	M
Na	4.4E+00
Al	1.1E-01
Cr	5.8E-03
Re	1.6E-03
B	1.1E-02
K	5.4E-03
NO_3	2.2E+00
NO_2	3.7E-01
OH	1.8E+00
CO_3	1.4E-01
SO_4	4.6E-02
C_2O_4	9.3E-03
Cl	4.6E-03

Table 2. Ingredients used to prepare the simulated salt solution.

Compound	**g / L**
Water	balance
KNO_3	0.55
$NaNO_3$	154.37
NaOH (50%)	142.4
$Al(NO_3)_3 \cdot 9H_2O$	42.01
$NaNO_2$	25.66
Na_2CO_3	14.73
Na_2SO_4	6.59
Na_2CrO_4	0.94
$Na_3PO_4 \cdot 12H_2O$	1.9
$Na_2C_2O_4$	1.24
H_3BO_3	0.71
NaCl	0.27

The ingredients and proportions in the cementitious materials and mixtures prepared for x-ray diffraction characterization are provided in Table 3. Each mix was prepared as a large batch in a chemical fume hood using a paddle mixer with the blade set about 2 cm above the bottom of a 2000 ml beaker. The cementitious reagents were premixed by shaking them in a sealed plastic bag. The liquid was added to the beaker before the mixer was turned on and the rotational speed was adjusted to about 250 revolutions per minute (rpm). The corner of the bag containing the cementitious reagents was cut, and the contents of the bag were slowly added to the solution. After all of the solid reagents were added, the slurry was mixed for 3 minutes at a paddle speed adjusted to form a vortex but minimize air entrapment. After mixing, each mixture was cast into multiple 70 mL plastic containers. The containers were filled completely and capped. After setting on the bench top for 3 days the samples were over packed in a plastic bag to which a damp cloth was added to provide a moisture curing environment in case the caps were breeched. All samples were cured at ambient laboratory conditions.

Table 3. Material prepared for x-ray-diffraction characterization.

Sample No.	Sample Description (Ingredients and Proportions)					Water to cementitious materials mass ratio
	Portland cement I/II	Ground Granulated Blast Furnace Slag (Grade 100)	Class F fly ash	ASTM Type 1 water	4.4 M Na Salt Waste Simulant	
	(g)					
448-1A, 1B, 1C	Anhydrous cement	--	--	--	--	NA
448-2A, 2B, 2C	--	Anhydrous slag	--	--	--	NA
448-3A, 3B, 3C	--	--	Anhydrous fly ash	--	--	NA
448-4A to 4G	500	--	--	300	--	0.60
448-5A to 5G	--	500	--	300	--	0.60
448-6A to 6G	--	--	500	300	--	0.60
448-7A to 7G	751	--	--	--	602	0.60
448-8A to 8G	--	751	--	--	602	0.60
448-9A to 9G	--	--	751	--	602	0.60
448-10A to 10G	150	601	--	--	602	0.60
448-11A to 11G	150	--	601	--	602	0.60
448-12A to 12G	--	375.5	601	--	602	0.60
448-13A to 13G	75	338	338	--	602	0.60

One sample of each material was sent to E. Pierce, Oak Ridge National Laboratory, Oak Ridge, TN, after curing for 28 days. The intent was to obtain x-ray diffraction powder patterns at the ORNL as a precursor to neutron diffraction analyses at the ORNL Spallation Neutron Source. The neutron diffraction analyses were to be arranged by E. Pierce.

In addition, D. M. Missimer, SRNL Analytical R&D Programs, performed x-ray diffraction analyses on identical samples cured for 14 months to evaluate the effect of curing time on the mineralogy. A Bruker DA Advance x-ray diffractometer with CuKα radiation (1.5405982 Å wave length) was used to generate the diffraction patterns. JADE x-ray analysis software from Materials Data Inc. was used to identify phases along with chemistry of the materials and information from the literature.

LITERATURE REVIEW

Portland cement, GGBFS and Class F fly ash, and pastes made from these ingredients and combinations of ingredients have been extensively characterized in the literature. Limited data on pastes made with salt solutions are available in the literature. The review presented in this report is intended to illustrate that portland cement, GGBFS, Class F fly ash, and blends of these ingredients are multi-phase materials which have differing and variable compositions. In addition hydration products of these materials and blends are also multiphase. In addition, the mineralogy of the hydrated phases depends on many factors including the mineralogy of the starting materials, bulk oxide compositions of ingredients and blends, amount of water available for hydration, temperature, time, and other environmental conditions.

Portland cement: ASTM C-150 does not identify proportions of the phases in portland cement. Instead, oxide chemical requirements are identified and a method of estimating phase proportions based on chemical analysis is provided. Phases and materials in Type I/II portland cement are listed in Table 4. Minor phases present in portland cement clinker may include: periclase (Mg) and sodium and potassium sulfate phases: arcanite, aphthitalite, and langbeinite.

Table 4. Portland cement mineralogy.

Phase	Cement Shorthand Terminology*
Cement clinker	
Ca_3SiO_5	C_3S Alite and polymorphs
Ca_2SiO_4	C_2S Belite, Larnite and polymorphs
$Ca_3A_2O_6$	C_3A
$Ca_2(Al_x,Fe_{1-x})_2O_5$ series	C_4AF $_{\text{where x = 0.5}}$ Ferrite
K_2SO_4	$K_2\boldsymbol{S}$ Arcanite
$(K,Na)_3Na(SO_4)_2$	$(K,N)_3N\boldsymbol{S}_2$ Aphthitalite
$(K_2Mg_2(SO_4)_3$	$K_2M_2\boldsymbol{S}_3$ Langbeninite
MgO	M Periclase
Interground material	
Gypsum $CaSO_4{\cdot}_2H_2O$	C***S***
Limestone (calcite $CaCO_3$ + mineral phases occurring in limestone)	C***C***
Grinding aids and particle dispersants	Inorganic: fly ash or slag (< 3%) [Stutzman, 2014] Organic: e.g., aliphatic amines, complex amines, glycol compounds, phenol and phenolic derivatives [Katsioti, et al. 2009]

* Cement notation uses capital letters of the first letter in the chemical symbol to indicate one mole of the oxide, e.g., C = CaO, A = Al_2O_3, S = SiO_2, M = MgO, F = Fe_2O_3, N = NaO, and H = H_2O. The letters C and S overlain with bars $\overline{C}$, $\overline{S}$ are used to represent SO_4^{2-} and CO_3^{2-} in conventional cement notation as are the bold italic letters ***C*** and ***S***.

Hydrated Portland Cement: Phases formed in Type I/II portland cement hydrated with potable water (water to cement (w/c) ratio of 0.4 to 0.6) and cured under ambient laboratory conditions are listed in Table 5. Hydrated portland cement consists of calcium-rich gels with a range of Ca/Si ratios, calcium hydroxide, and one or more hydrated calcium aluminate phases. The C-S-H gels are often described as non-cross linked tobermorite- and jennite-like structures [Myers, 2013].

Inner product C-S-H forms within the space originally occupied by either alite or belite grains in the portland cement and also in space originally occupied by slag grains. The Ca/Si of the inner C-S-H hydration product is typically between 1.5 and 2.0 [Taylor, 1997]. Outer product C-S-H forms in the space originally filled by water. It typically has a lower Ca/Si ratio than the inner product C-S-H. In hydrated portland cement paste the outer product typically contains a mixture of inter-grown portlandite and AFm and AFt phases and has a fibrous morphology. Blends of portland cement and GGBFS result in a foil-like C-S-H morphology rather than a fibrous like morphology.

The inner product C-S-H typically displays a dense, coarse morphology. Rims of particles oriented perpendicular to the original grain boundaries are often formed around the alite, belite, and slag grains which may persist for years. The inner product can also contain laths or platelets of AFm and relicts of AFt needles [Richardson and Groves, 1992, and Taylor, 1997]. AFt phases have the general formula

$[Ca_3(Al,Fe)(OH_6)]\cdot X_3\cdot xH_2O$, where X represents one formula unit of a doubly charged anion or 2 formula units of a singly charged anion.

AFm phases are layered double hydroxides (LDHs) and have a distorted layered structure derived from portlandite, $Ca(OH)_2$. The entire family of AFm phases is often grouped together as the hydrocalumite phases. In the simplest structures, one Ca^{2+} ion in three is typically replaced by Al^{3+} or Fe^{3+}. The Ca : Al ratio is 2:1 and SO_4^{2-}, CO_3^{2-}, or OH^- occupy the anion positions. The cation layers alternate with layers containing anions and H_2O. AFm phases typically found in hydrated portland cements and blended cements include: hydroxy AFm, $4CaO\cdot Al_2O_3\cdot$13-19 H_2O, hemicarboaluminate, monocarboaluminate, Friedel's salt, $3CaO\cdot Al_2O_3\cdot CaCl_2\cdot xH_2O$, and stratlingite, a calcium aluminate silicate hydrate. A large number of AFm minerals occur naturally and can sequester both multivalent anions and cations.

Table 5. Hydrated Portland cement mineralogy (w/c = 0.4 to 0.6; ambient temperature curing).

Phase	Composition
C-S-H (inner product)	Ca/Si ~ 2
C-S-H (outer product)	Ca/Si ~ 1.5 to 1.1
Portlandite	Ca(OH)2
Ettringite (Aft)	$Ca_6Al_2(SO_4)_3(OH)_{12}\cdot 26H_2O$
Monosulfoaluminate (AFm)	$Ca_4Al_2(SO_4)(OH)_{12}\cdot 6H_2O$
Monocarboaluminate*	$Ca_4Al_2(CO_3)(OH)_{13}\cdot 5.5H_2O$
Hemicarboaluminate*	$Ca_4Al_2(CO_3)_{0.5}(OH)_{12}\cdot 5H_2O$
Hydrogarnet	$Ca_3[Al(OH)_6]_2$

* The presence of inter-ground fine limestone in the current portland cements is likely to produce carbonate hydrates.

Ground Granulated Blast Furnace Slag: GGBFS is produced by quenching molten iron slag in water or steam (wet quenching), then drying and grinding it into a fine powder. The main components of blast furnace slag are CaO (30-50%), SiO_2 (28-38%), Al_2O_3 (8-24%), and MgO (1-18%). GGBFS is 90 to 100 % glass. The amount of glass depends on the cooling rate and temperature at which the quenching is initiated. GGBFS used in concretes and mortars is specified in ASTM C989. Li, et. al, 2011 concluded that GGBFS glass is separated into two phase: a Ca-rich phase and a Si-rich phase that approximates akermanite ($Ca_2Mg[Si_2O_7]$). Most of the Si is distributed around Mg and calcium is associated with both Si and Al. Depending on the characterization techniques and slag preparation, micro- to nano-crystallites have been reported in GGBFS slag glasses.[1]

Alkali Activated Slag (AAS): GGBFS is a glass which is slow to react with water. However, in the presence of alkali and water, it is activated and forms hydrated cementitious phases. Examples of phases formed when GGBFS is activated by different chemicals are provided in Table 6. The main hydration product of Na(OH) activated slag is a sodium substituted calcium-aluminum-silicate hydrate, C(N)-A-S-H, typically with a lower Ca/Si ratio (1.1 to 1.2, i.e. close to the ratio in unreacted slag) and higher Al/Si ratio than the C-S(A)-H resulting from portland cement hydration [Richardson and Groves, 1992]. The aluminum substituted gel is charge balanced with alkali and the gel structure can be described as tobermorite-like with the possibility of some cross-linking between the tobermorite chains [Myers, et.al, 2013]. The C-S-H gel formed in hydrated cement-slag mixtures is reported to be more like that formed from portland cement hydration (no cross-linking) and forms along with calcium hydroxide [Taylor, 1997].

[1] Sulfur in slag is often assumed to be associated with calcium in the glass structure because crystallized slags contain minor amounts of reduced sulfur as CaS with varying amounts of Mg and Fe substituted for Ca.

Table 6. Hydrated Slag Mineralogy.

Phase	Taylor, H.F.W., Cement Chemistry, 2nd ed., 1997		Fernandez-Jimenez, A. and F. Puertas, J. Am Ceram. Soc. 86(8) 1389-94 (2003)		
	Cement Activated Slag (1:1)	**Alkali Activated Slag (3.5-5.5M NaOH)**	**NaOH Activated Slag**	**$NaCO_3$ Activated Slag**	**Na Silicate Activated Slag (water glass)**
C-S-H	Ca/Si ~1.55 Al/Ca ~ 0.09	C-S-H(I) relatively highly ordered Ca/Si ~1.1 to 1.2 Al/Ca ~0.19 Al in C-S-H substituted exclusively in bridging sites of dreierketten w/mean chain length 4.83 tetrahedron	C-S-H with dreierkette-type (3 chain) structure shows high Q2 Si values indicative of long linear chains but no Q3 Si values, i.e., low strength. Semi-crystalline, Foil like morphology Ca/Si = 0.9-1.0 (lower than starting slag) Na/Al = 2.0-2.22 Tetrahedral condensation ratios are higher in NaOH AAS and Water glass activated than in Na_2CO_3 AAS indication Al is incorporated in tet chains with charge balanced by Na+ (TEM/EDS).	C-S-H shows low Q3 Si values. Med. Strength Semi-crystalline, Foil like morphology Ca/Si = 0.9 to 1.0 (lower than in the starting slag)	C-S-H with highly condensed anions, Si in Q2 and Q3 sites which favors formation of cross-linked structures that result in increased strength
$CaCO_3$	Not mentioned	Not mentioned	Yes	Yes	--
Hydrotalcite-type phase $Mg_6Al_2(CO_3)(OH)_6 \cdot 4(H_2O)$	Mg/Al = 3 to 2.5 if Fe replaces Al	--	Yes	Yes	--
AFm phase	--	possible	--	--	--
AFm Carboaluminate phase(s) of the C4A*C*3H11-Type	--	--	Yes	Yes	--
Zeolites	Formed at temp. > 120 ºC in hydrated systems	Formed at temp. > 120 ºC in hydrated systems	Zeolite formation requires high Al/Si and low Ca/Si	Not mentioned	--
$Na_2Ca(CO_3)_2 \cdot 0.5\ H_2O$	--	--	--	Yes	--

Poorly ordered hydrotalcite-like phase, $Mg_6Al_2(OH)_{16}CO_3 \cdot 4H_2O$, is also characteristic of GGBFS hydration. Hydrotalcite is structurally related to brucite in a way that is analogous to AFm phases being related to portlandite and is a layered double hydroxide. Some of the Mg ions may be replaced by Al^{3+} and Fe^{3+} and the charge balanced by anions which together with H_2O molecules occupy interlayer sites [Taylor, 1998]. The layer thicknesses are similar to that of the AFm phases and it is difficult to distinguish between the two groups by x-ray diffraction if only the basal reflections are observed.

Other phases that may form from alkali activated slag include: Fe-rich cubic hydrogarnet, $Ca_3[Al(OH)_6]_2$ and one or more AFm phases, $Ca_2(Al,Fe)(OH)_6]\cdot X \cdot xH_2O$ where X is one formula unit of a singularly charged anion or half of a formula unit of a doubly charged anion. Other phases which can form include: $C_4AH_{13,}$tetracalcium aluminum hydrate; $C_2ASH_{8,}$ stratlingite, $Ca_2Al_2(SiO_2)(OH)_{10}\cdot 2.5(H_2O)$; and/or hydrocalumite, $Ca_4Al_2(OH)_{12}(CO_3,OH)_2 \cdot 4H_2O$ [Chen and Brouwers, 2007 and Taylor, 1997].

The type of alkali used to activate the slag has an effect on the reaction products. Na(OH) activation of GGBFS results in poorly-ordered C-S-H with a foil like morphology and Ca/Si = 0.9 to 1.0 (lower than in the starting slag) and Na/Al of 2.0 to 2.22. This gel has a dreierkette-type structure (three chain structure). The relatively long linear chains correlate with mechanical strength. The mean chain length is about 8 tetrahedra [Fernandez-Jimenez and Puertas, 2003, Schilling et. al, 1994 and Richardson et. al 1982]. Other phases found in NaOH activated slag included: calcite, hydrotalcite, and carboaluminates.

Based on ^{29}Si and ^{27}Al magic-angle spinning (MAS) nuclear magnetic resonance (NMR) spectroscopy, Na_2CO_3 activated slag also results in poorly-ordered C-S-H with a foil like morphology and lower Ca/Si ratio than that formed from NaOH activation. The strengths of the Na_2CO_3 activated slag gels are reported to be higher than those formed from NaOH activated slag. The highest strengths are reported to be obtained from sodium silicate (water glass) activation slag. The C-S-H formed from the highly condensed anions in the case of sodium silicate favored formation of cross-linked structures that contributed to increased mechanical strength [Fernandez-Jimenez and Puertas, 2003].

Class F Fly Ash: Class F fly ash is a byproduct of burning bituminous coal in a coal-fired electric and steam producing power plants. The molten fly ash material solidifies while suspended in the exhaust gases and is collected by electrostatic precipitators or filter bags before the gases are discharged. Since the particles solidify rapidly, fly ash particles are generally cenospheres, (single or joined spheres), or plerospheres (spheres with in spheres), and range in size from < 0.5 μm to 300 μm. Due to the rapid cooling, most of the fly ash is amorphous (glass). Crystalline phases in fly ash are either refractory phases in the coal or formed from minerals in the coal. These phases are typically incorporated in the glass cenospheres and plerospheres. In summary, fly ash is a heterogeneous material. Most of the material is a glass which may contain quartz, mullite, iron oxides(hematite and/or maghemite), cristobalite, anhydrite, free lime, periclase, calcite, rutile and anatase. Examples of fly ash mineralogy are provided in Table 7. Detailed structural analysis of the amorphous material in Class F fly ash suggests that the glass is not homogeneous at the time it is quenched [Bumrongjaroen, et.al, 2007].

Hydrated Class F Fly Ash: Class F fly ash is mostly inert when exposed to water and air. However, when calcite, $CaCO_3$, is detected in Class F fly ash it is an indication that the ash contained a small amount of CaO which typically hydrates and then carbonates. Class F fly ash is pozzolanic and reacts with calcium, aluminum, and water to produce poorly ordered cementitious material.[2]

[2] Geopolymers can also be formed from Class F fly ash when activated by alkali solutions such as sodium hydroxide or sodium silicate (water glass).

Table 7. Class F fly ash mineralogy.

Phase	Taylor, H. F. W. Cement Chemistry, 2nd ed. , 1997	Bumrongjaroen, W., I. S. Muller, and I. L. Pegg, 2007 VSL-07R520X-1	McCarthy, G. J., 1988
Glass	Cu Kα peaks around 22-23° 2θ	71.9 wt. % Mullite-rich ~ 53.6 Class F glass ~ 24.1 Spinel rich ~ 12.8 Low-silica glass ~ 5.8 Class C glass ~ 2.0 Quartz rich ~ 1.7	x
Mullite $Al_6Si_2O_{13}$ **prisms in glass**	x	18.9	x
Quartz SiO_2 **prisms in glass or angular particles**	x	6.7	x
K_2SO_4 **particles adhering to spheres**	x	--	--
$CaSO_4$ **particles adhering to spheres**		Trace	--
Hematite Fe_2O_3 **particles adhering to spheres or separate particles**	x	1.07	x
Magnetite Fe_3O_4 **particles adhering to spheres or separate particles**	x	1.13	x
Ferrite Spinel Sub Mg, Al, Ti, Ni, Cr	--	0	Al substituted for Fe and could be misidentified as magnetite [Wingurn, R. S., S.S. Lerach, G. J. McCarthy, 2000 JCPDS Data Advances in X-ray Analysis V. 43, p.350]
Carbon **Porous particles**	x	Not determined	Not determined
Cenospheres (hollow spheres)		Not evaluated	Not evaluated
Plerospheres (spheres filled with other spheres or particles)		Not evaluated	Not evaluated

RESULTS

X-ray powder diffraction is one of several complimentary techniques for identifying phases in solid materials. In this study, an attempt was made to identify changes in the mineralogy starting with the anhydrous cement, slag, and fly ash and progressing to characterization of these materials hydrated with water and also with sodium salt solution. This information was used to help interpret and characterize the reaction products of selected blends of these cementitious materials as the result of hydration in water and salt solution was also performed.

Anhydrous starting materials: Phases identified in the anhydrous Type II portland cement, Grade 100 GGBFS, and carbon burn-out (CBO) Class F fly[3] ash are listed in Table 8. The mineralogy of these materials is consistent with the phases reported in the literature. The x-ray diffraction techniques used in this study can detect minor amounts (greater than about 3 weight percent) of crystalline phases in the samples. Broad low intensity peaks in the powder x-ray diffraction patterns are indicative of anhydrous and hydrated poorly ordered silicate- based phases.

The portland cement, Sample 1A, contained alite ($Ca_3SiO_{5)}$, larnite ($Ca_2SiO_{4)}$, a ferrite phase ($Ca_2(Al,Fe)O_5$) and calcite ($CaCO_3$). Neither gypsum nor anhydrite was detected in the x-ray patterns although it is known to be inter-ground with the cement to control the initial hydration reactions. Since this cement contained a low amount of tricalcium aluminate ($Ca_3A_2O_6$) which was below the detection limit for the x-ray diffraction technique used, the amount of calcium sulfate required to control the tricalcium aluminate hydration reaction was probably also low.

The Grade 100 slag, Sample 2A, was predominantly a silicate glass (non-crystalline material) containing a trace amount of akermanite ($Ca_2Mg[Si_2O_7]$), a refractory calcium magnesium silicate phase that formed during the slag production. Calcite was also detected in the x-ray diffraction pattern and was assumed to form as the result of lime in the slag reacting with CO_2 in the air.

The Class F fly ash, Sample 3A, also consists of glassy material (non-crystalline) which contains mullite ($Al_6Si_2O_{13}$) and quartz (SiO_2). The mullite formed as a refractory aluminum silicate phase when clays in the coal were melted and were subsequently crystallized. The quartz is a residual phase from the coal itself.

Hydration of starting materials in water: Phases detected in the cementitious starting materials hydrated in water are also listed in Table 8. These samples were cured in sealed containers at room temperature for 2 and 14 months. The amount of non-crystalline or poorly ordered C-S-H in the cement + water samples, 4A and 4G, may have increased between 2 and 14 months but quantitative x-ray diffraction was not perfomed. Ettringite, an AFt phase, $Ca_6Al_2(SO_4)_3(OH)_{12}\cdot 26H_2O$, calcium aluminum sulfate hydrate, and a trace amount of an AFm phase, probably monosulfoaluminate were detected in the x-ray patterns.

Poorly ordered material, interpreted as unreacted anhydrous glass, was the predominant phase in the GGBFS samples 5A and 5G cured in water for 2 and 14 months, respectively. However, some hydration of the slag in water seems to have occurred in the 14 month old sample as indicated by detection of a

[3] Carbon Burn Out consists of combusting residual carbon in fly ash to produce a consistent, low carbon (< 2.5 wt. %) high quality pozzolan. The drivers for CBO are to control the amount of carbon in fly ash to levels acceptable for construction applications and to eliminate ammonia contamination of the ash. Introduction of low NOx burners in recent years at coal fired power plants has resulted in increased levels of residual carbon in the ash. Also ammonia injection is used in some plants to enhance electrostatic precipitator performance and is being applied in selective catalytic reduction and selective non-catalytic flue gas treatment systems to meet the new more stringent NOx off gas standards. (Removal of ammonia is considered for fly ash if it contains more than about 50 -100 ppm if it is to be used in concrete applications.)

Table 8. Phases identified in XRD powder patterns of anhydrous cementitious reagents and individual hydrated materials and the corresponding International Center for Diffraction Data (ICDD) database card numbers.

Material	Sample No. (Cure Time)	Glass NCS	Hyd-rated NCS	CSH 034-0002	11Å Al-Tober-morite 019-0052	Hydro-talcite 041-1428	Hydro-calumite AFm 031-0245	Ettring-ite AFt 041-1451	Port-landite 004-0733	Ca_3SiO_5 049-0442	Ca_2SiO_4 033-0902, 033-0302	Brown-millerite $Ca_2(Al,Fe)O_5$ 042-1469	Gyp-sum 033-0311	Quartz SiO_2 046-1045	Mullite $Al_6Si_2O_{13}$ 015-0776	Aker-manite 035-0592	Calcite $CaCO_3$ 005-0586	Natra-tine $NaNO_3$ 036-1474	Comments
Type II cement	1A	--	--	--	--	--	--	--	--	X	X	X	--	--	--	--	x	--	
Grade 100 slag	2A	X	--	--	--	--	--	--	--	--	--	--	--	--	--	?	?	--	
Class F Fly ash	3A	X	--	--	--	--	--	--	--	--	--	--	--	X	X	--	--	--	
Type II Cement + Water	4A (2 mo.)	--	?	?	?	x	--	X	X	--	?	--	--	--	--	--	--	--	Bad pattern
	4G (14 mo.)	--	X	--	?	x	--	X	X	X	--	--	?	--	--	--	--	--	? Calcium iron sulfate hydrate 040-0292
Slag + Water	5A (2 mo.)	X	?	?	?	--	--	--	--	--	--	--	--	--	--	--	--	--	
	5G (14 mo.)	X	?	--	--	x	?	--	--	--	--	--	--	--	--	x	x	--	
Fly ash + Water	6A (2 mo.)	X	--	--	--	--	--	--	--	--	--	--	--	X	X	--	--	--	
	6 (14 mo.)	Not evaluated																	

X = Several major peaks identified. x = Peaks identified with low relative intensity. ? = Peaks overlap other peaks, no unique peak identified, Tr = Identified based on small peaks and chemistry. -- = Not identified.

small amount of a hydrotalcite-type phase[4] or a mixture of hydrotalcite and hydrocalumite (AFm). C-S-H may be present in the sample but SEM/EDX or other techniques are required to determine whether it formed. Calcite and possibly akermanite, present in the unreacted slag, were also detected in the GGBFS hydrated in water for 2 and 14 months.

Class F fly ash was essentially inert in the presence of water (samples 6A) which was cured for 2 months. The same phases present in the unhydrated the CBO Class F fly ash were detected in this sample, i.e. glass, and the refractory phases mullite and quartz.

Hydration of Starting Materials in 4.4 M Na Salt Solution: Phases detected in samples of the starting reagents, Type I/II portland cement, GGBFS, and CBO Class F fly ash, hydrated in 4.4 M Na salt solution are listed in Table 9. The phases detected by x-ray diffraction for the cement hydrated in salt solution samples (7A and 7E) included: poorly ordered C-S-H gel phase, portlandite, an AFm phase (calcium aluminate sulfate hydrate), unreacted larnite, and nitratine ($NaNO_3$) a component in the salt solution / pore solution.

Based on the powder pattern phase identifications, hydration of GGBFS in 4.4 M Na solution (Samples 8A and 8G) resulted in formation of fairly well crystallized material C-S-H I and aluminum substituted 11 Å tobermorite, in addition to a hydrotalcite-like phase and / or a mixture of hydrotalcite- and hydrocalumite-like phases. Some material, either unreacted glass or poorly ordered C-(Al)-S-H, may also be present in samples cured for 2 and 14 months. Additional characterization techniques are required to determine if residual slag or poorly ordered C-(Al)-S-H or other amorphous phases are present. Quartz and a calcium iron oxide were identified based on d-spacings but were not detected in the slag and could not have formed during hydration. Addition work is being performed to obtain reasonable phase identification for those d-spacings attributed to those diffraction peaks.

No additional crystalline phases were detected in the Class F fly ash cured in 4.4 M Na salt solution (Samples 9A and 9F). Residual mullite and quartz were detected in the x-ray diffraction patterns along with poorly ordered or amorphous material which is probably a mixture of silicate glass and hydrated glass. Exposure to caustic solutions results in partial to complete dissolution of the fly ash cenospheres.

Hydration of Blends in Salt Solution: Mineralogies of the blended binders are listed in Table 10. Samples 10 A and B were prepared with a 1 : 3 mixture by weight of cement : slag and were hydrated with 4.4 M Na salt solution for 2 and 14 months, respectively. Both samples contained fairly well ordered C-S-H I and aluminum substituted 11 Å tobermorite in addition to more than one AFm-type phase, either hydrotalcite or a mixture of hydrotalcite and hydrocalumite. Poorly ordered C-S-H may be present but could not be differentiated from residual slag glass. Larnite (from the anhydrous cement) and akermanite and calcite (from the anhydrous slag) were also detected in trace amounts. $NaNO_3$ was also present in both x-ray diffraction patterns and in all patterns for materials hydrated with the sodium salt solution. The samples cured for 2 and 14 months had similar phase assemblages.

Samples 11A and 11G were prepared with a 1 : 3 mixture of cement : Class F fly ash. These samples were hydrated for 2 and 14 months with 4.4 M Na salt solution. The reaction product in both of these samples was primarily poorly ordered C-S-H. Residual larnite, mullite, and quartz were also detected in both samples in addition to $NaNO_3$. The 2 and 14 month old samples do indicate changes in the calcium aluminate (sulfate) hydrate phases as a function of curing time. More detailed characterization is required to determine the composition and structure of these layered hydrates.

[4] Hydrotalcite-type phases are layered double hydroxides (LDHs) with metal cations in the main layers and anion and water in the interlayers. They are structurally related to brucite, $Mg(OH)_2$. The general formula is $Mg_6Al_2(OH)_{16}$.

Table 9. Phases identified in XRD powder patterns of individual cementitious materials hydrated with 4.4 M Na salt solution and the International Center for Diffraction Data (ICDD) Database Card Numbers.

Material	Sample No. Cure Time (mo)	Silicate Glass NCS	C-S-H Hydrated NCS	CSH I 034-0002	11Å Al-Tobermorite 019-0052	Hydrotalcite 041-1428	Hydrocalumite 031-0342	Ettringite 041-1451	Hydrogarnet	Portlandite 004-0733	Ca_3SiO_5 049-0442	Ca_2SiO_4 033-0902	$Ca_2(Al,Fe)O_5$ 042-1469	Gypsum 033-0311	Quartz 046-1045	Mullite 015-0776	Akermanite 035-0592	Calcite 005-0586	$NaNO_3$ 036-1474	Comments
Cement + Salt Solution	7A (2)	--	X	--	--	--	x 049-0457	--	--	X	--	x	--	--	--	--	--	--	X	
	7E (14)	--	X	--	--	--	x 049-0457	--	--	X	--	x	--	--	--	--	--	--	X	
Slag + Salt Solution	8A (2 mo.)	?	X	X	X	X	?	--	--	--	--	--	--	--	X	--	--	--	X	
	8B (14 mo.)	?	X	X	X	X	?	--	--	--	--	--	--	--	X	--	--	--	X	
Fly ash + Salt Solution	9A (2 mo.)	X	--	--	--	--	--	--	--	--	--	--	--	--	X	X	--	--	X	Low Counts
	9F (14 mo.)	X	--	--	--	--	--	--	--	--	--	--	--	--	X	X	--	--	X	X

X = Several major peaks identified. x = Peaks identified with low relative intensity. ? = Peaks overlap other peaks, no unique peak identified, Tr = Identified based on small peaks and chemistry, -- = Not identified.

Table 10. Phases identified in XRD powder patterns of blends of cementitious materials hydrated with 4.4 M Na salt solution and the International Center for Diffraction Data (ICDD) Database Card Numbers.

Material	Sample No. Cure Time (mo)	Glass NCS	Hyd-rated NCS	CSH I 034-0002	11Å Al-Tober-morite 019-0052	Hydro-talcite 041-1428	Hydro-calu-mite 031-0245	Ettring-ite 041-1451	Hydro-garnet	Port-landite 004-0733	Ca_3SiO_5 049-0442	Ca_2SiO_4 033-0902, 033-0302	$Ca_2(Al, Fe)O_5$ 042-1469	Gyp-sum	Quartz 046-1045	Mullite 015-0776	Aker-manite 035-0592	Calcite 005-0586	$NaNO_3$ 036-1474	Comments
Cement + Slag + Salt Solution	10A (2 mo.)	?	X?	X	X	X	?	--	--	--	x	x	--	--	--	--	x	x	X	061-0217 $CaAl_2O_4 10{\cdot}H_2O$
	10B (14 mo.)	?	X?	X	X	X	?	--	--	--	--	x	--	--	--	--	x	x?	X	061-0217 $CaAl_2O_4 10{\cdot}H_2O$
Cement + Fly Ash + Salt Solution	11A (2 mo.)	?	X	--	--	--	x	--	--	--	--	x	--	--	X	X	--	--	X	
	11C (14 mo.)	?	X	--	--	--	--	?	--	--	--	x	--	--	X	X	--	--	X	Possibly 2 new phases K_2SO_4, $NaAl(AlSi_3)O_{10}(OH)_2$
Slag + Fly Ash + Salt Solution	12A (2 mo.)	?	X	--	--	--	X	--	--	--	--	--	--	--	X	X	--	--	X	
	12F (14 mo.)	?	X	--	--	--	X	--	--	--	--	--	--	--	X	X	--	--	X	
Cement + Slag + Fly Ash + Salt Solution	13A (2 mo.)	?	X	--	--	X	??	--	--	--	--	--	--	--	x	x	?	?	X	
	13G (14 mo.)	?	X	?	--	X	??	--	--	--	--	--	--	--	X	X	?	x	X	

X = Several major peaks identified. x = Peaks identified with low relative intensity. ? = Peaks overlap other peaks, no unique peak identified, Tr = Identified based on small peaks and chemistry, -- = Not identified.

Samples 12A and 12F were prepared with a 2 : 3 mixture of slag and fly ash and cured for 2 and 14 months, respectively. These samples contained poorly ordered C-S-H and one or more layered double hydroxide phases (hydrotalcite, hydrocalumite, carboaluminate phase or a mixture of these phases) in addition to residual mullite, quartz, and $NaNO_3$. Crystalline C-S-H I and Al substituted tobermorite were not formed in this blend.

Samples 13A and 13G were prepared with a 10 : 45 : 45 mixture of cement : slag : fly ash and were cured for 2 and 14 months, respectively. These samples contained mainly poorly ordered C-S-H and hydrotalcite. Trace amounts of CSH I and / or Na substituted 11 Å tobermorite (2-theta of 6-7º) and one or more layered double hydroxide phases (hydrotalcite, hydrocalumite, or a mixture of these phases), residual mullite, quartz, calcite, and possibly akermanite in addition to $NaNO_3$.

DISCUSSION

The mineralogy of the samples cured for 2 and 14 months is determined by the mineralogy and bulk composition of the hydraulic and pozzolanic components and the chemistry of the mixing water or aqueous salt solution. The compositions of the cement, slag, and fly ash used to prepare the paste samples analyzed in this study are provided in Attachment 2. The values for five oxides, CaO, MgO, Al_2O_3, Fe_2O_3, and SiO_2, which together make up about 90 or more of the mass percent of each binder material were averaged and normalized. See Tables 11 and 12, respectively.

The sums of the normalized basic oxides were divided by sums of the acidic oxides, i.e., (CaO and MgO) / (SiO_2, Al_2O_3, and Fe_2O_3) for individual ingredients (cement, slag, and fly ash) and for four blends all of which were hydrated with the 4.4 M Na salt solution. Results are tabulated in Table 12 and plotted in Figure 1. (Aluminum as aluminate in the salt solution was not included in the calculation.)

Based on the (CaO + MgO) / (SiO_2 + Al_2O_3) ratios the mineralogy of the three individual ingredients and four blends hydrated with the alkaline salt solution can be loosely grouped into four categories shown below:

(CaO + MgO) / (SiO_2 + Al_2O_3)	**Binder Phases**
> 2	Poorly ordered C-S-H gel (Ca/Si > 1.5) + $Ca(OH)_2$
~ 1 to 1.3	Ordered CSH I (Ca/Si ~ 1.1 to > 1.5) + 11 Å tobermorite
~ 0.3 to 0.5	Poorly ordered C-S-H gel
~ 0.05	Si dissolution

The (CaO + MgO) / (SiO_2 + Al_2O_3) ratios of the ternary blends currently used and being considered for DOE salt waste forms fall in the 0.3 to 0.5 range and result in poorly ordered C-S-H (possibly with Na and Al substitution) matrix phases. Mineralogy is related to some physical properties, such as, dimensional stability as a function of temperature and moisture conditions, porosity, hydraulic conductivity, and durability. Consequently, mineralogy of waste form matrices is important to performance and evolution as a function of changing conditions and time. Mineralogy is also important for selecting appropriate thermodynamic data for long term equilibrium calculations used in chemical degradation scenarios.

Table 11. Major oxide results for cement, slag and Class F fly ash.

Oxide	Cement A	Cememt B	Cement Ave	Slag A	Slag B	Slag Ave	Fly Ash A	Fly Ash B	Fly Ash Ave
	Wt. %	Wt. %	Wt. %	Wt. %	Wt. %	Wt. %	Wt. %	Wt. %	Wt. %
CaO	64.4	64.4	**64.4**	35.8	36.7	**36.3**	2.4	2.4	**2.4**
MgO	1.19	1.2	**1.2**	13.3	12.9	**13.1**	1.5	1.5	**1.5**
Al_2O_3	5.25	5.1	**5.2**	7.8	8.1	**8.0**	24.9	24.8	**24.9**
Fe_2O_3	3.72	3.9	**3.8**	0.3	0.3	**0.3**	12.8	12.8	**12.8**
SiO_2	19.2	19.7	**19.5**	39.8	39.2	**39.5**	48.4	47.9	**48.2**
TOTAL	93.76	94.3	94.0	97.0	97.2	97.1	90.1	89.4	89.8

Table 12. Normalized selected oxides for starting materials and four blends.

Oxide	Normalized Blend 10 cement: 45 slag: 45 fly ash	Normalized Blend 25 cement: 75 fly ash	Normalized Blend 25 cement: 75 slag	Normalized Blend 38 slag: 62 fly ash	Normalized Cement	Normalized Slag	Normalized Class F Fly Ash
	Wt. %	Wt. %	Wt. %	Wt. %	Wt. %	Wt. %	
CaO	24.9	19.2	45.1	15.8	68.5	37.3	2.7
MgO	7.0	1.6	10.4	6.2	1.2	13.5	1.7
Al_2O_3	16.7	22.2	7.5	20.3	5.5	8.2	27.7
Fe_2O_3	7.0	11.8	1.3	9.0	4.1	0.3	14.3
SiO_2	44.5	45.4	35.7	48.7	20.7	40.7	53.6
TOTAL	100.0	100.0	100.0	100.0	100.0	100.0	100.0
Oxide Ratios							
(CaO + MgO) ÷ (SiO_2 +Al_2O_3)	0.52	0.31	1.29	0.32	2.66	1.04	0.05
(CaO + MgO) ÷ (SiO_2+ Al_2O_3+ Fe_2O_3)	0.47	0.26	1.25	0.28	2.30	1.03	0.05
CaO ÷ (SiO_2 + Al_2O_3)	0.41	0.28	1.04	0.23	2.61	0.76	0.03

Shaded ratios are plotted in Figure 1.

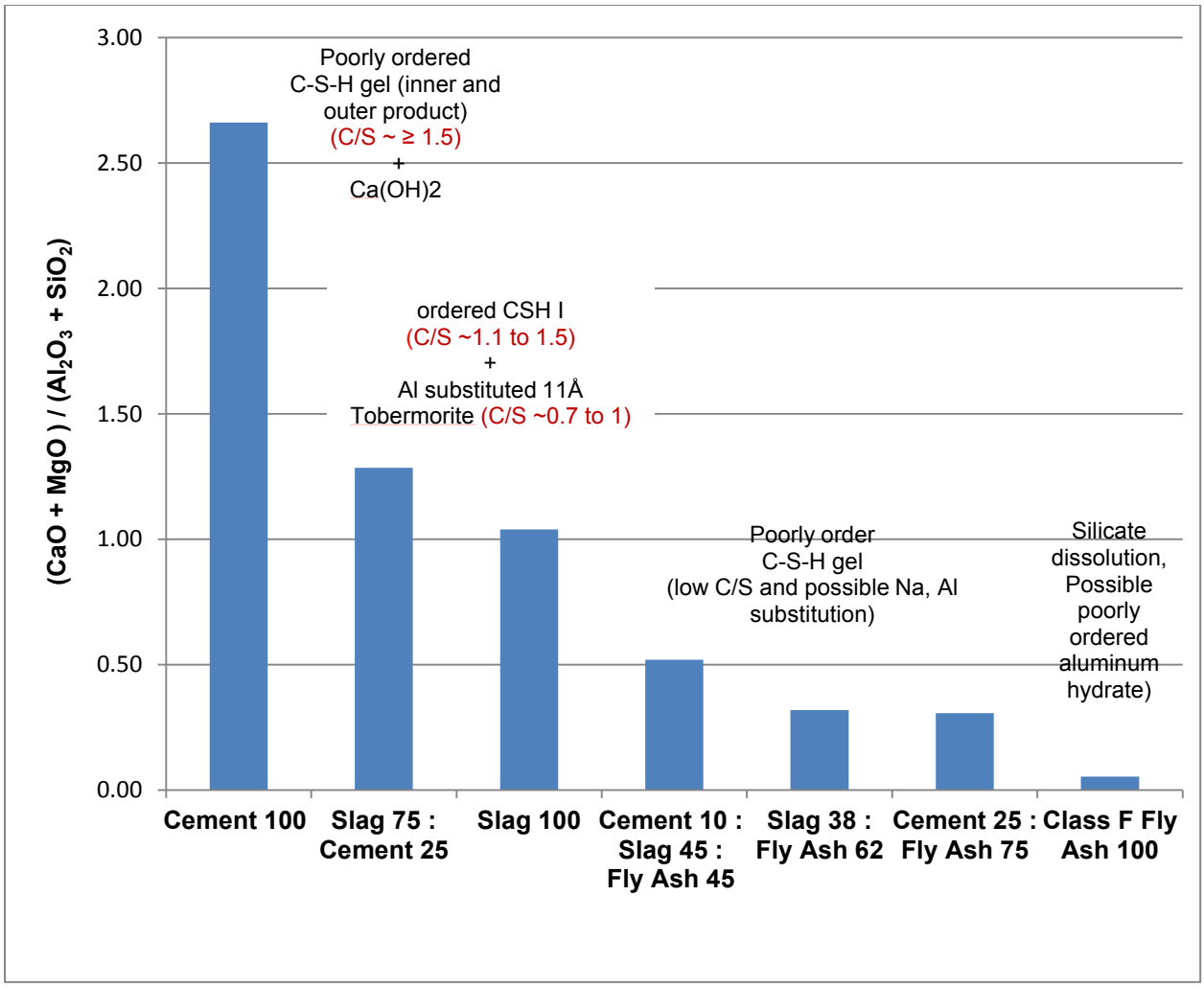

Figure 1. Calcium silicate hydrate phases in binders hydrated with 4.4 M Na salt solution as a function of (CaO + MgO) / (Al_2O_3 + SIO_2) ratio.

CONCLUSIONS

The mineralogy of the reaction products for materials and blends of materials hydrated with caustic 4.4 M Na salt solution depended on the mineralogy and proportions of the cementitious ingredients and the bulk oxide compositions of the mixtures. Poorly ordered /amorphous C-S-H was detected in mixtures of cement and slag, cement and fly ash, slag and fly ash and the waste form blend containing cement, slag, and fly ash when hydrated with caustic 4.4 M Na salt solution. Only the neat slag and cement + slag mixture hydrated with caustic 4.4 M Na salt solution contained fairly well crystallized C-S-H I and Al substituted 11 Å tobermorite.

Hydrotalcite and hydrocalumite-like phases and mixtures of these LDH phases were present in the all of the blended samples. However the proportions of these phases and probably their compositions varied. Not surprisingly, the phase assemblage in the 10:45:45 blend of cement : slag : fly ash resembled that of the slag : fly ash blend.

The mineralogy of the hydrated materials evaluated did not change significantly between 2 months and 14 months curing in sealed containers. Characterization of samples cured for much longer times is

recommended. Both drying conditions and curing in the presence of excess water are expected to result in changes in the mineralogy.

Cement hydrated for up to 14 months in water and up to 14 months in salt solution contained, poorly ordered C-S-H, portlandite ($Ca(OH)_2$), and an AFm phase. The AFm phase identified in the salt solution hydrated sample was a sodium aluminate sulfate. Ettringite, an Aft phase ($Ca_6(Al,Fe)_2(OH)_{12}(SO_4)_3.26H_2O$) was identified in the water hydrated cement sample but not in the salt solution hydrated sample. Unreacted larnite (Ca_2SiO_4) from the cement and $NaNO_3$ from the salt solution were detected in the salt solution hydrated sample.

Class F fly ash showed no significant reaction with water in the samples hydrated for 2 and 14 months. Hydration of the fly ash in salt solution resulted in dissolution of some of the glassy material as indicated by residual mullite "baskets". The only crystalline phases detected in the x-ray diffraction patterns were the refractory phases, mullite and quartz, present in the anhydrous fly ash.

GGBFS did not hydrate or hydration was very limited after 2 months in water based on x-ray diffraction results. However, after 14 months, a small amount of LDH phase (hydrotalcite and / or hydrocalumite (AFm) or a mixture) was detected in the x-ray pattern. In contrast, activation of the slag in the 4.4 M Na salt solution resulted in formation of fairly well crystallized C-S-H I and Al substituted 11 Å tobermorite ($Ca_5Si_3Al(OH)O_{17}\cdot 5H_2O$). These two ordered calcium silicate hydrates were detected in slag and mixtures of slag and cement hydrated with 4.4 M Na salt solution.

The mineralogy of the cured cementitious material influences the physical properties (strength, stiffness, etc.) of the cured material due to the degree of polymerization (chain length) and tetrahedron arrangement. Information about the mineralogy of hydrated cementitious materials and blends of these ingredients is needed to design waste form matrices, select ingredients and make adjustments in material proportions. Information presented in this report is an initial step in developing phase diagrams for the hydrated systems in which caustic sodium salt solutions are used as the hydration fluid for waste forms.

REFERENCES

ASTM C150-12. "Standard Specification for Portland Cement," 2012, ASTM International, West Conshohochen, PA, 19428.

ASTM C989-14. "Standard Specification for Slag Cement for Use in Concrete and Mortars," 2014, ASTM International, West Conshohochen, PA, 19428.

ASTM D1193-11. "Standard Specification for Reagent Water," 2011, ASTM International, West Conshohochen, PA, 19428.

Bumrongjaroen, W., I. S. Muller, and I. L. Pegg, 2007. "Characterization of glassy phase in fly ash from Iowa State University", VSL-07R520X-1, Vitreous State laboratory, Washington DC, 2007.

Chen, W, H. J. H. Brouwers, 2007. "The hydration of slag, Part 1: Reaction models for alkali-activated slag," J. Mater. Sci. 42:428-443.

Chen, W, H. J. H. Brouwers, and Z. H. Shui, 2007. "Three-dimensional computer modeling of slag cement hydration," J. Mater. Sci., 42:9595-9610.

Katsioti, M, P.E. Tsakiridis, P. Giannatos, Z.Tsibouki, and J. Marinos, 2009. "Characterization of various cement grinding aids and their impact on grindability and cement performance," Construction and Building Mat., 23(5):1954-1959.

Keppeler, J.G. and W.T.Frady, 2009. "Carbon burn-out: commercialization and experience update," http:/www.pmiash.com/cbo/acaa01paper.html.

Kirkpatrick, R. J., P. Yu, X Hou, and Y. Kim, 1999. "Interlayer structure, anion dynamics, and phase transitions in mixed-metal layered hydroxides: Variable temperature 35Cl NMR spectroscopy of hydrotalcite and Ca-Aluminate hydrate (hydrocalumite)," Am. Min. 4:1186-1190.

Langton, C.A. and H.H. Burns, 2012. "Characterization of phases in Savannah River Site saltstone using neutron diffraction at the ORNL Spallation Neutron Source, Task Technical and Quality Assurance Plan (TT/QAP)", SRNL-RP-2012-00448, Savannah River National Laboratory, Aiken, SC 29801.

Langton, C.A., D.S. Kosson, A.C. Garrabrants, and K.G. Brown, 2009. "Reference cases for us in the Cementitious Barriers Partnership Project," SRNL-STI-2009-00005, WM Symp, 2009.

Li, Chao, H. Sun, and L.Li, 2011. "Glass phase structure of blast furnace slag," *Advanced Materials Research*, 168-170:3-7.

Matschei, T., B. Lothenbach, and F.P. Glasser, 2007. The AFm phase in portland cement," Cem. And Concrete Res. 37:118-130

McCarthy, G. J., 1988. "X-ray powder diffraction for studying the mineralogy of fly ash." Fly ash and Coal Conversion By-products: Characterization, Utilization and Disposal , Mat. Res. Soc. Proc., 113:75-86.

Myers, R. J., S. A. Bernal, R.S.Nicolas, and J. L. Provis, 2013. "Generalized structural description of calcium-sodium aluminosilicate hydrate gels: The cross-linked substituted tobermorite model," Langmuir, 29:5294-45406.

Palmer, S.J., T. Nguyen, and R. L. Frost, 2009. "Hydrotalcites and their role in coordination of anioins in Bayer liquors: Anion binding in layered double hydroxides," Coordination Chemistry Reviews 253(1-2):250-267.

Richardson, I.G. and G. W. Groves, 1992. "Microstructure and microanalysis of hardened cement pastes involving ground granulated blast-furnace slag," J. Mater. Sci. 27:6204-6212.

Stutzman, P., 2014. Personal communication.

Taylor, H. F. W, 1997. Cement Chemistry, 2nd ed., Thomas Telford, NY, NY.

Zhang, M and E. J. Reardon, 2003. "Removal of B, Cr, Mo, and Se from wastewater by incorporation into hydrocalumite and ettringite," Environ. Sci. Technol., 37(13):2947-295.

Attachment 1. X-Ray Diffraction Powder Patterns

Materials Data Inc., JADE 20/10 software was used to analyze the diffraction patterns. Due to the complex patterns and presence of poorly ordered and amorphous material in a few cases the software identified refractory phases which could not be present.

Anhydrous Cementitious materials

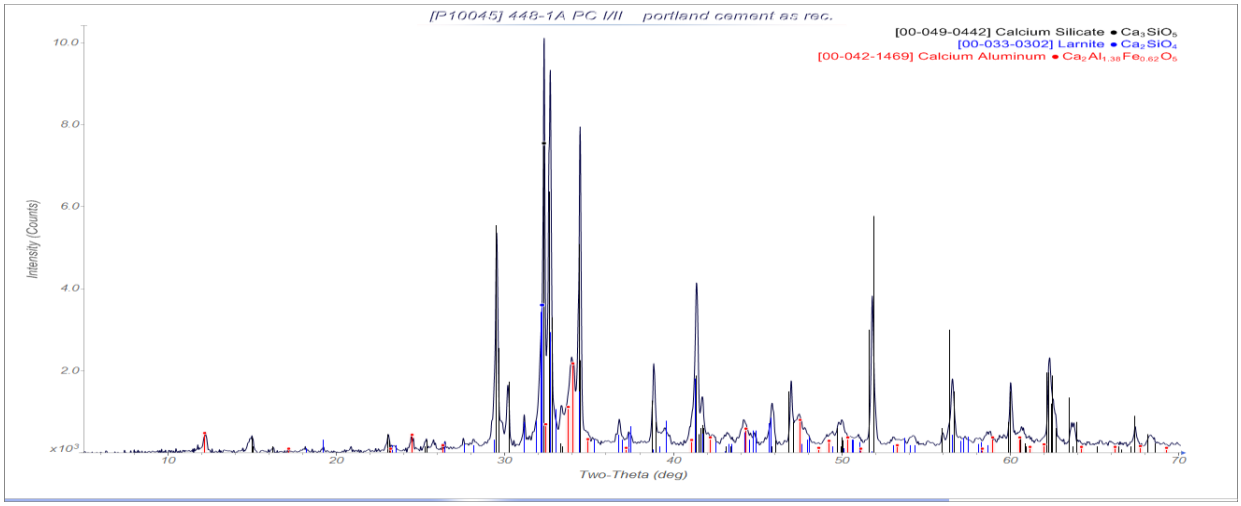

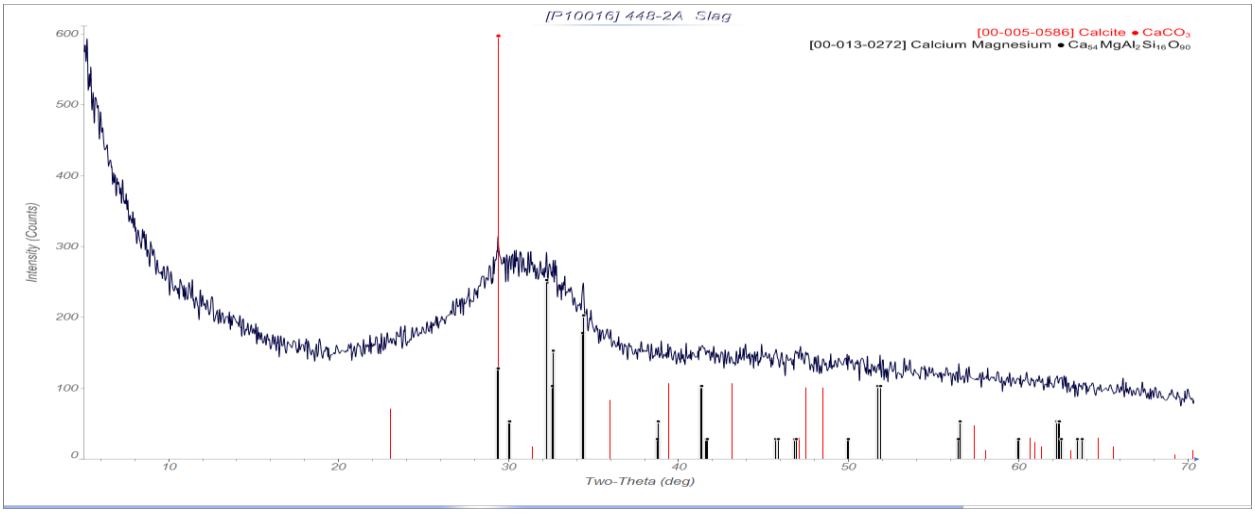

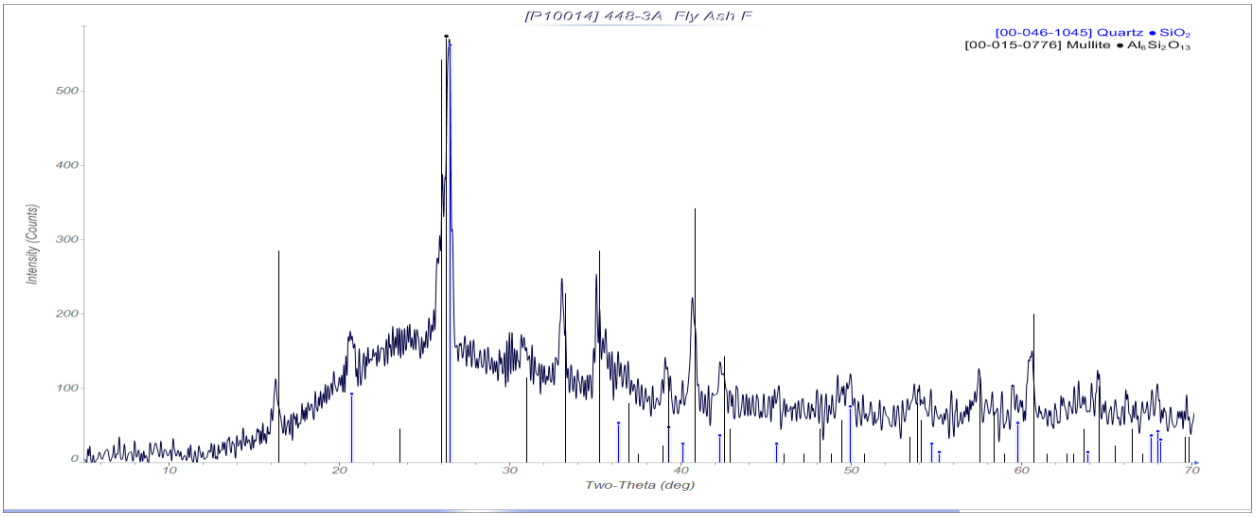

Water Hydrated Cementitious Reagents

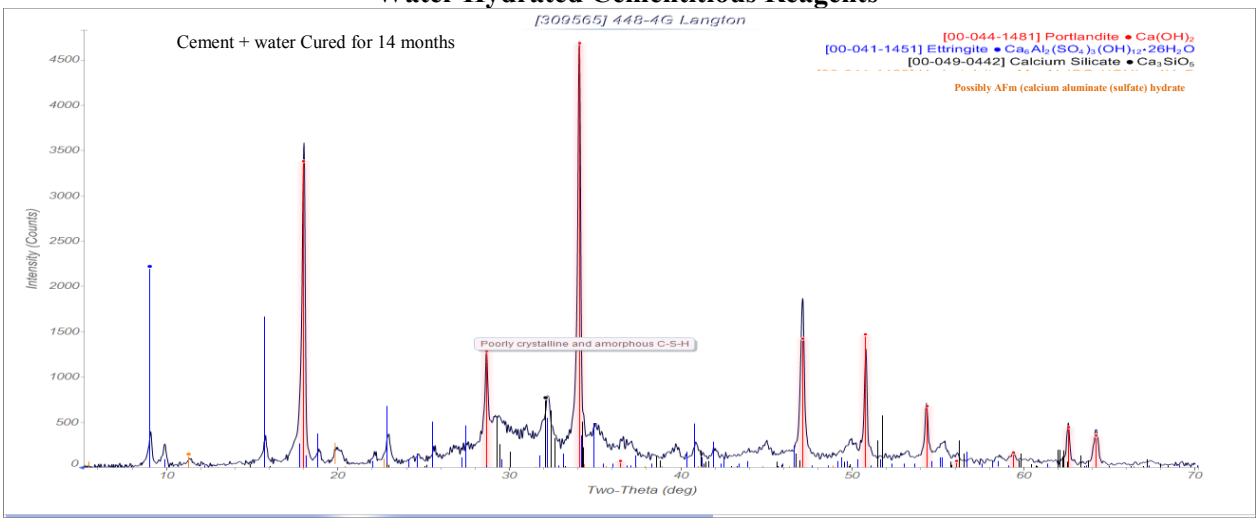

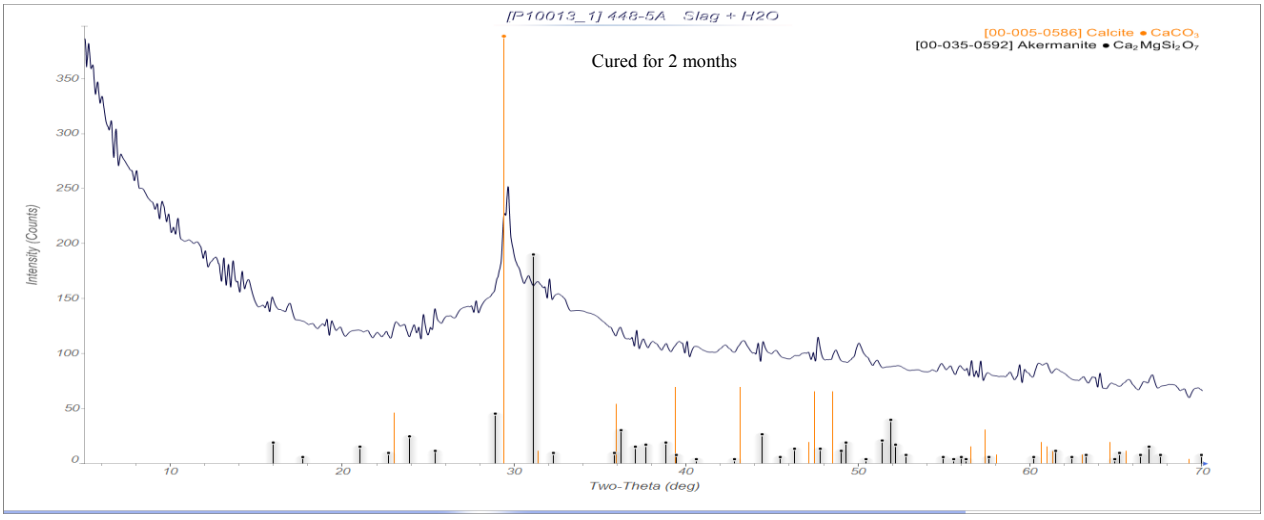

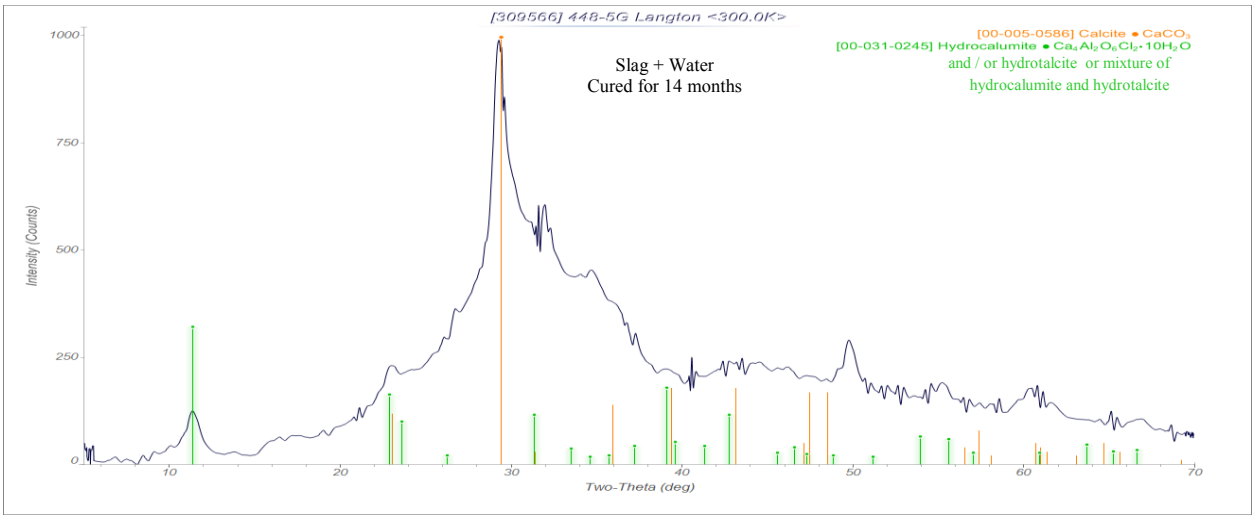

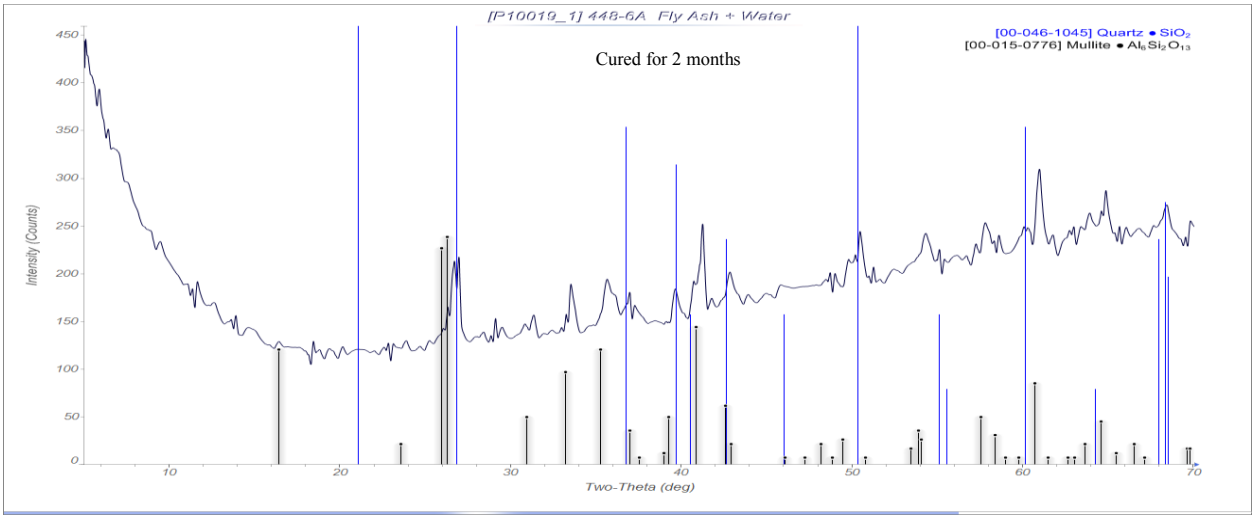
[P10019_1] 448-6A Fly Ash + Water
Cured for 2 months
[00-046-1045] Quartz • SiO2
[00-015-0776] Mullite • Al6Si2O13
Intensity (Counts)
Two-Theta (deg)
0
50
100
150
200
250
300
350
400
450
10
20
30
40
50
60
70

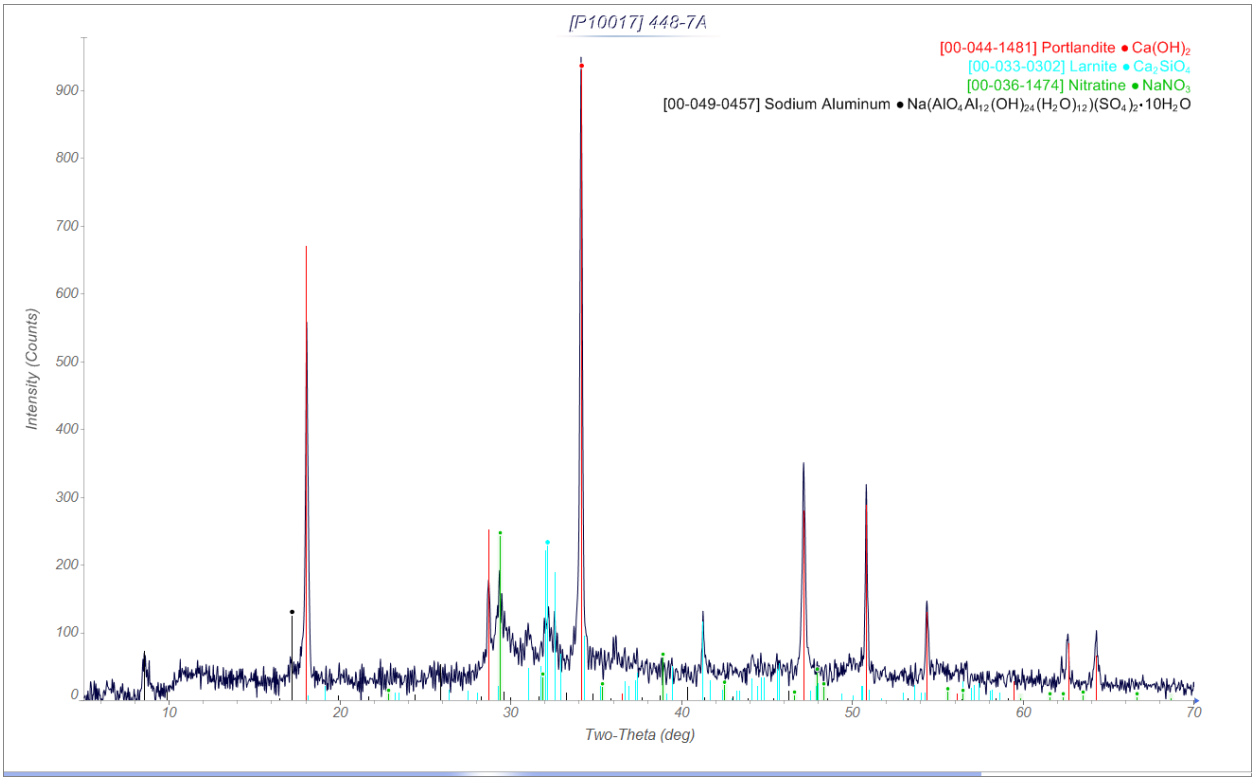
[P10017] 448-7A
[00-044-1481] Portlandite • $Ca(OH)_2$
[00-033-0302] Larnite • Ca_2SiO_4
[00-036-1474] Nitratine • $NaNO_3$
[00-049-0457] Sodium Aluminum • $Na(AlO_4Al_{12}(OH)_{24}(H_2O)_{12})(SO_4)_2 \cdot 10H_2O$
Intensity (Counts)
Two-Theta (deg)

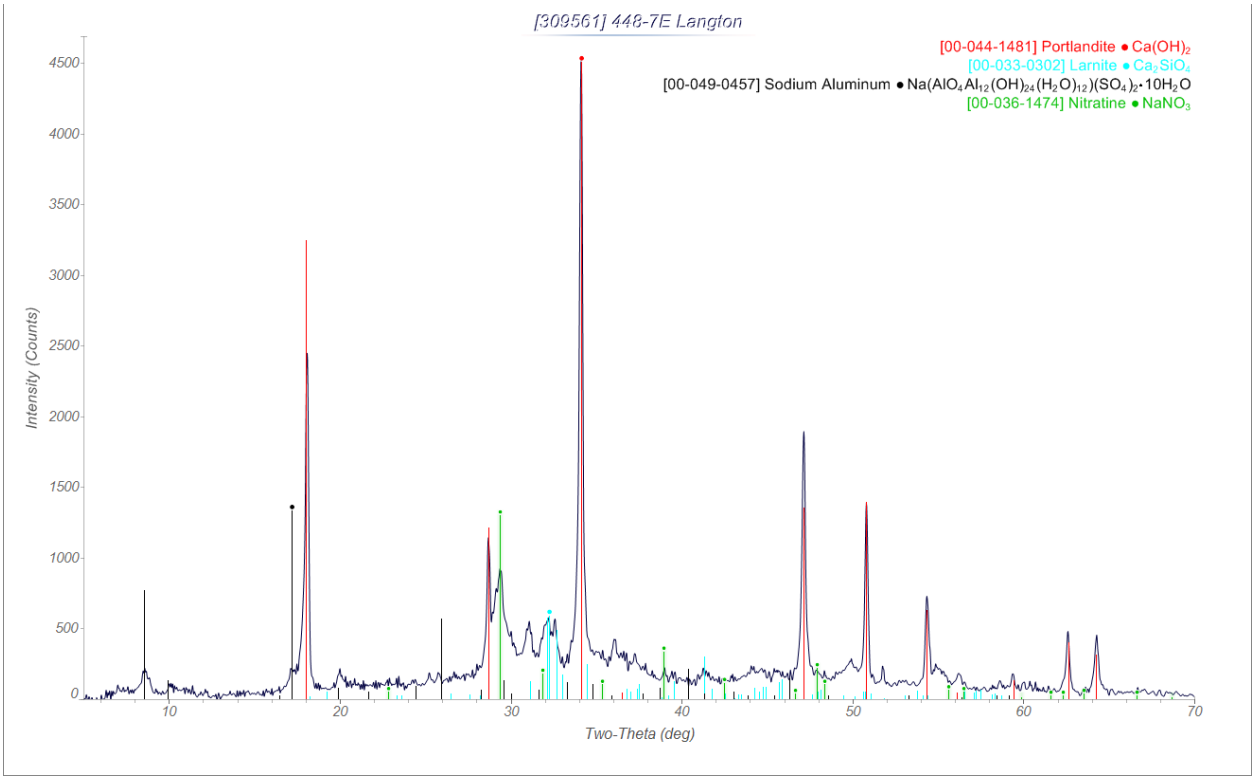
[309561] 448-7E Langton
[00-044-1481] Portlandite • $Ca(OH)_2$
[00-033-0302] Larnite • Ca_2SiO_4
[00-049-0457] Sodium Aluminum • $Na(AlO_4Al_{12}(OH)_{24}(H_2O)_{12})(SO_4)_2 \cdot 10H_2O$
[00-036-1474] Nitratine • $NaNO_3$
Intensity (Counts)
Two-Theta (deg)

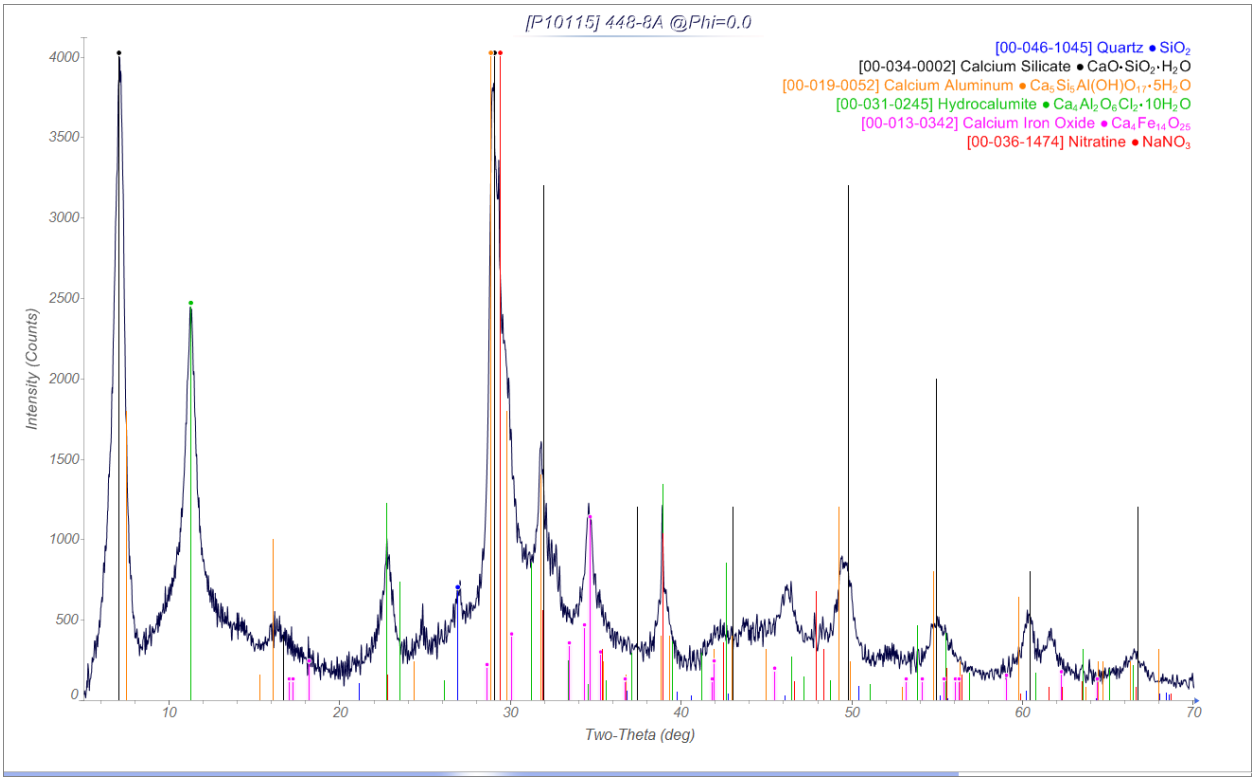
[P10115] 448-8A @Phi=0.0
[00-046-1045] Quartz • SiO2
[00-034-0002] Calcium Silicate • CaO·SiO2·H2O
[00-019-0052] Calcium Aluminum • Ca5Si5Al(OH)O17·5H2O
[00-031-0245] Hydrocalumite • Ca4Al2O6Cl2·10H2O
[00-013-0342] Calcium Iron Oxide • Ca4Fe14O25
[00-036-1474] Nitratine • NaNO3
Intensity (Counts)
Two-Theta (deg)

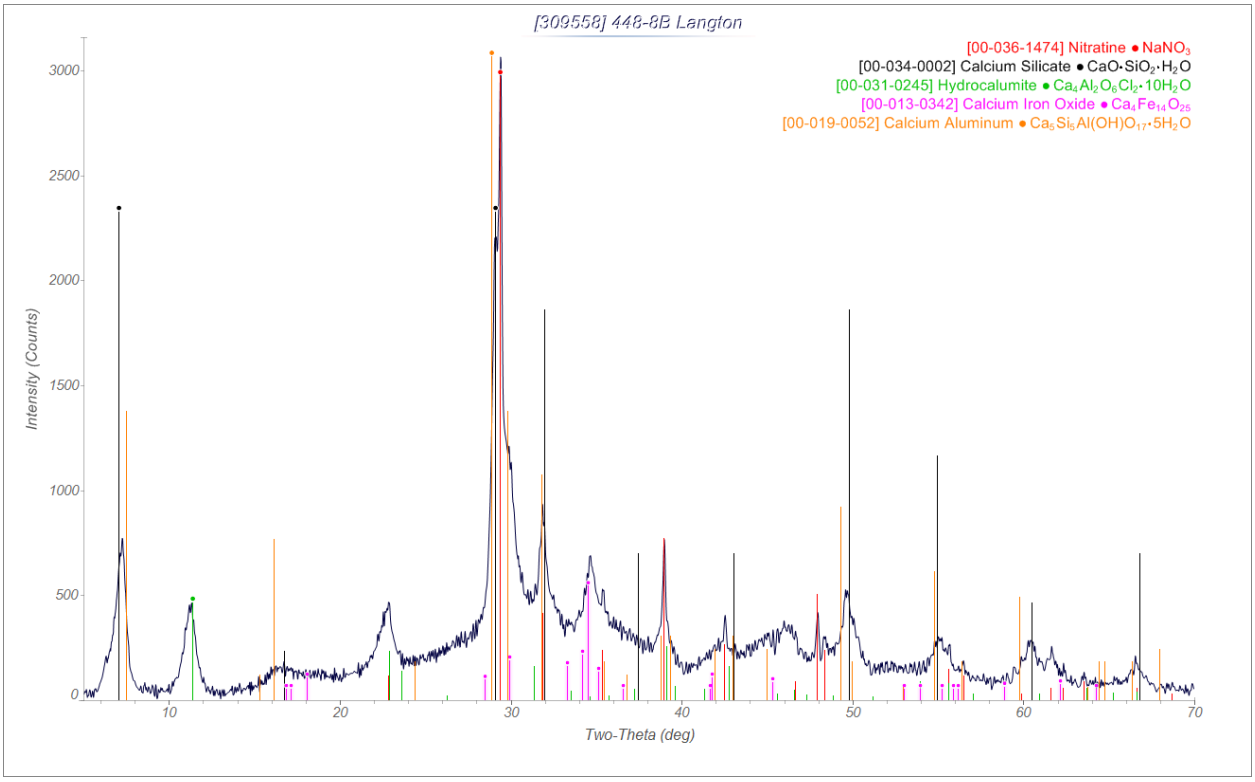
[309558] 448-8B Langton
[00-036-1474] Nitratine • NaNO3
[00-034-0002] Calcium Silicate • CaO·SiO2·H2O
[00-031-0245] Hydrocalumite • Ca4Al2O6Cl2·10H2O
[00-013-0342] Calcium Iron Oxide • Ca4Fe14O25
[00-019-0052] Calcium Aluminum • Ca5Si5Al(OH)O17·5H2O
Intensity (Counts)
Two-Theta (deg)

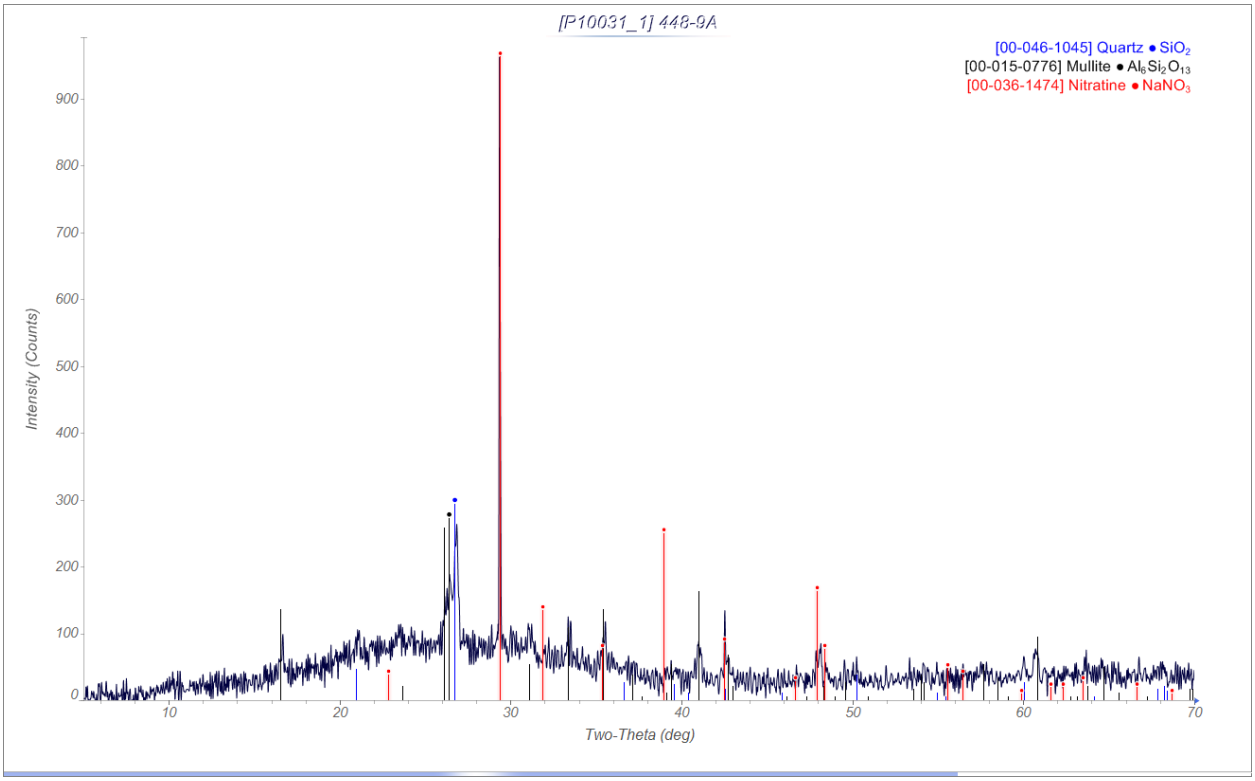
[P10031_1] 448-9A
[00-046-1045] Quartz • SiO2
[00-015-0776] Mullite • Al6Si2O13
[00-036-1474] Nitratine • NaNO3
Intensity (Counts)
Two-Theta (deg)

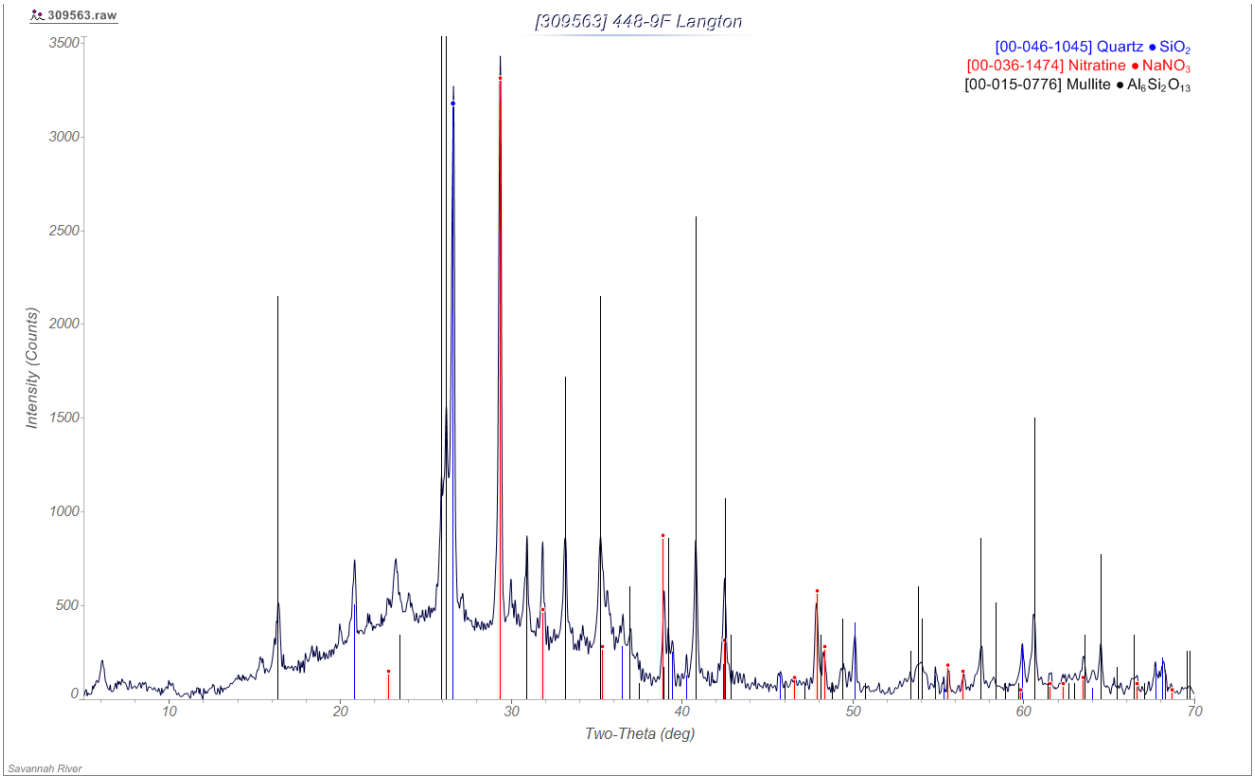
309563.raw
[309563] 448-9F Langton
[00-046-1045] Quartz • SiO2
[00-036-1474] Nitratine • NaNO3
[00-015-0776] Mullite • Al6Si2O13
Intensity (Counts)
Two-Theta (deg)
Savannah River

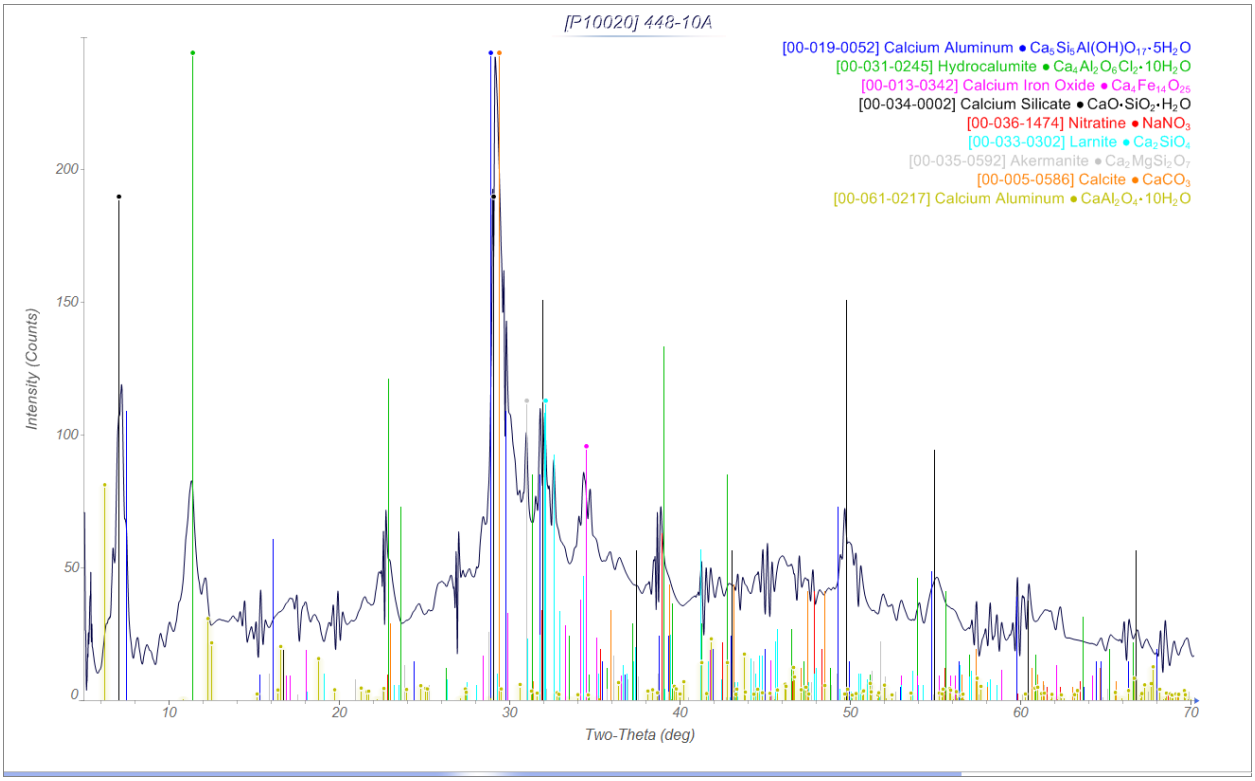
[P10020] 448-10A
[00-019-0052] Calcium Aluminum • $Ca_5Si_6Al(OH)O_{17}·5H_2O$
[00-031-0245] Hydrocalumite • $Ca_4Al_2O_6Cl_2·10H_2O$
[00-013-0342] Calcium Iron Oxide • $Ca_4Fe_{14}O_{25}$
[00-034-0002] Calcium Silicate • $CaO·SiO_2·H_2O$
[00-036-1474] Nitratine • $NaNO_3$
[00-033-0302] Larnite • Ca_2SiO_4
[00-035-0592] Akermanite • $Ca_2MgSi_2O_7$
[00-005-0586] Calcite • $CaCO_3$
[00-061-0217] Calcium Aluminum • $CaAl_2O_4·10H_2O$
Intensity (Counts)
Two-Theta (deg)

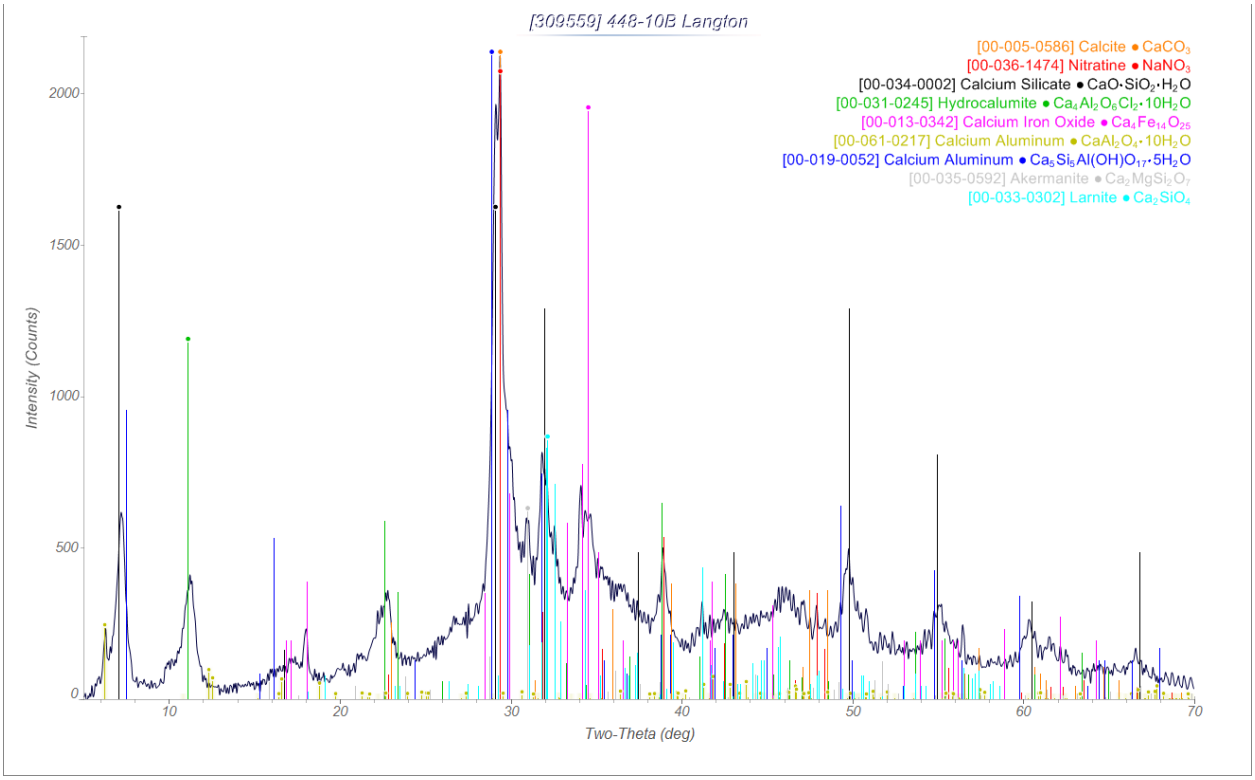
[309559] 448-10B Langton
[00-005-0586] Calcite • $CaCO_3$
[00-036-1474] Nitratine • $NaNO_3$
[00-034-0002] Calcium Silicate • $CaO·SiO_2·H_2O$
[00-031-0245] Hydrocalumite • $Ca_4Al_2O_6Cl_2·10H_2O$
[00-013-0342] Calcium Iron Oxide • $Ca_4Fe_{14}O_{25}$
[00-061-0217] Calcium Aluminum • $CaAl_2O_4·10H_2O$
[00-019-0052] Calcium Aluminum • $Ca_5Si_6Al(OH)O_{17}·5H_2O$
[00-035-0592] Akermanite • $Ca_2MgSi_2O_7$
[00-033-0302] Larnite • Ca_2SiO_4
Intensity (Counts)
Two-Theta (deg)

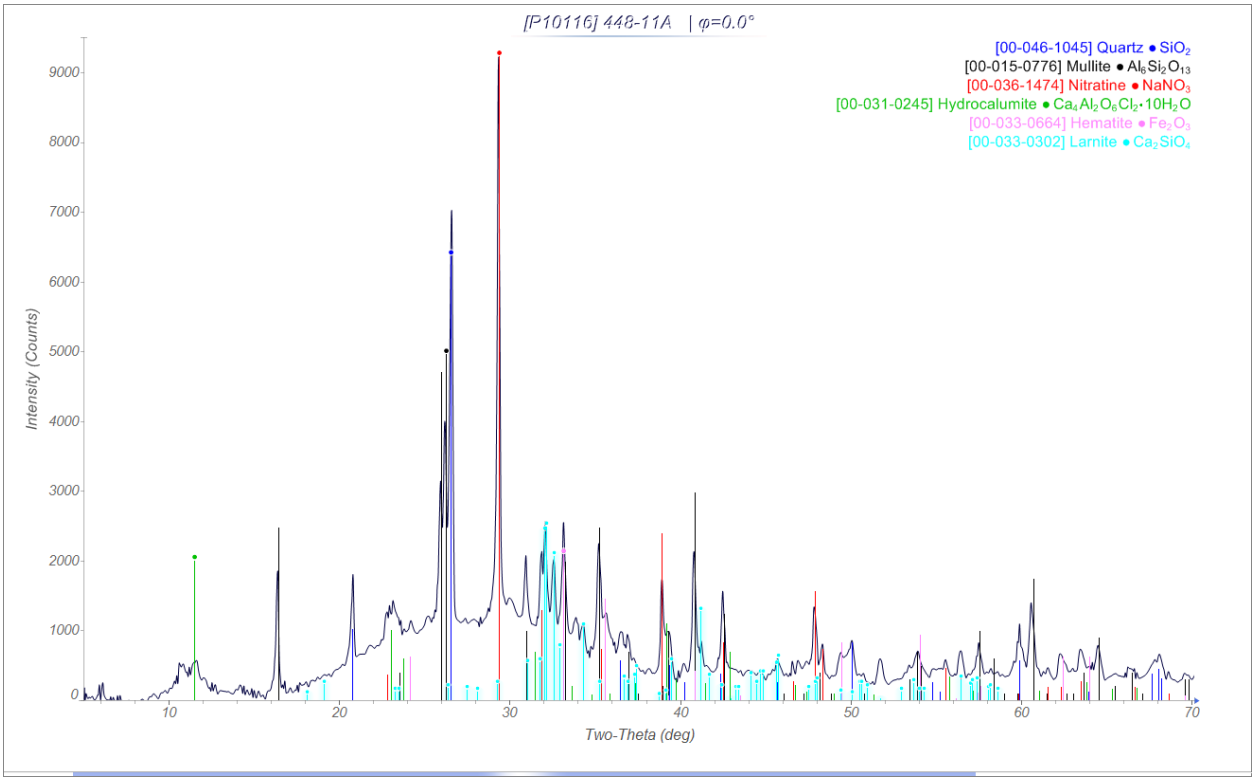
[P10116] 448-11A | φ=0.0°
[00-046-1045] Quartz • SiO2
[00-015-0776] Mullite • Al6Si2O13
[00-036-1474] Nitratine • NaNO3
[00-031-0245] Hydrocalumite • Ca4Al2O6Cl2·10H2O
[00-033-0664] Hematite • Fe2O3
[00-033-0302] Larnite • Ca2SiO4
Intensity (Counts)
Two-Theta (deg)

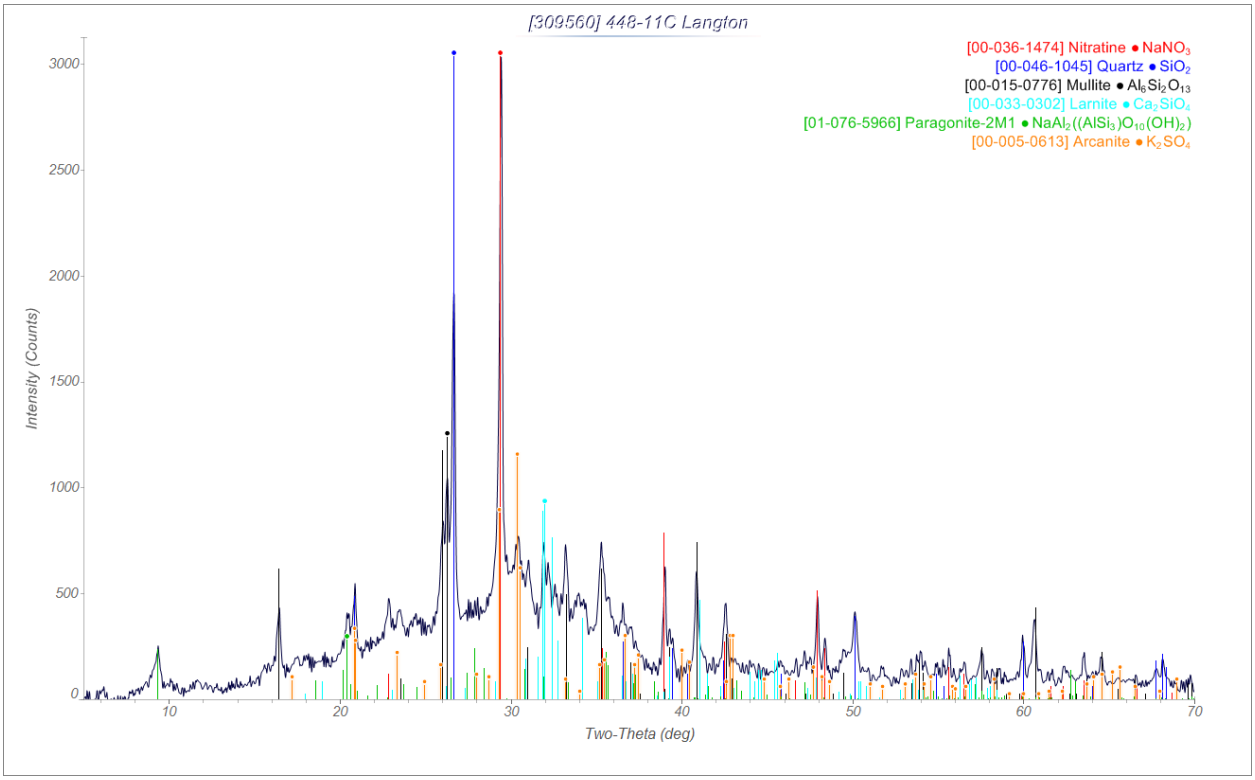
[309560] 448-11C Langton
[00-036-1474] Nitratine • NaNO3
[00-046-1045] Quartz • SiO2
[00-015-0776] Mullite • Al6Si2O13
[00-033-0302] Larnite • Ca2SiO4
[01-076-5966] Paragonite-2M1 • NaAl2((AlSi3)O10(OH)2)
[00-005-0613] Arcanite • K2SO4
Intensity (Counts)
Two-Theta (deg)

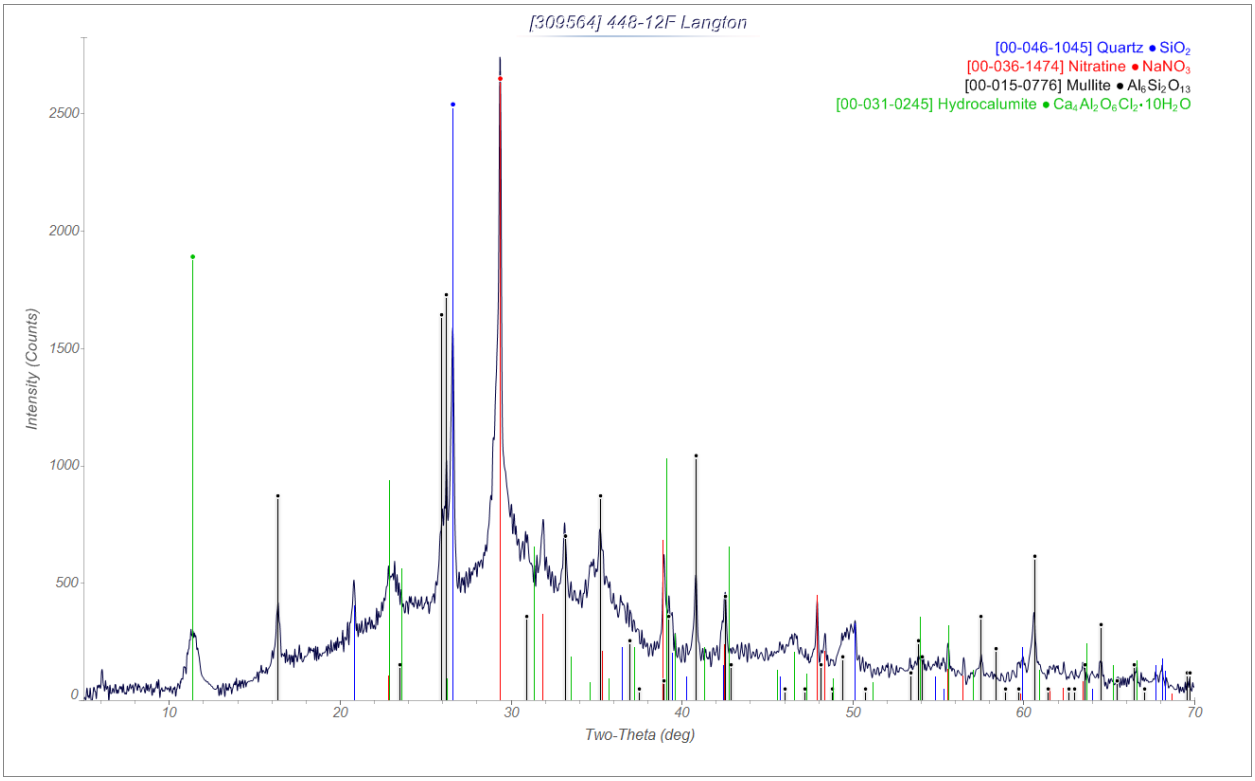
[309564] 448-12F Langton
[00-046-1045] Quartz • SiO2
[00-036-1474] Nitratine • NaNO3
[00-015-0776] Mullite • Al6Si2O13
[00-031-0245] Hydrocalumite • Ca4Al2O6Cl2·10H2O
Intensity (Counts)
Two-Theta (deg)

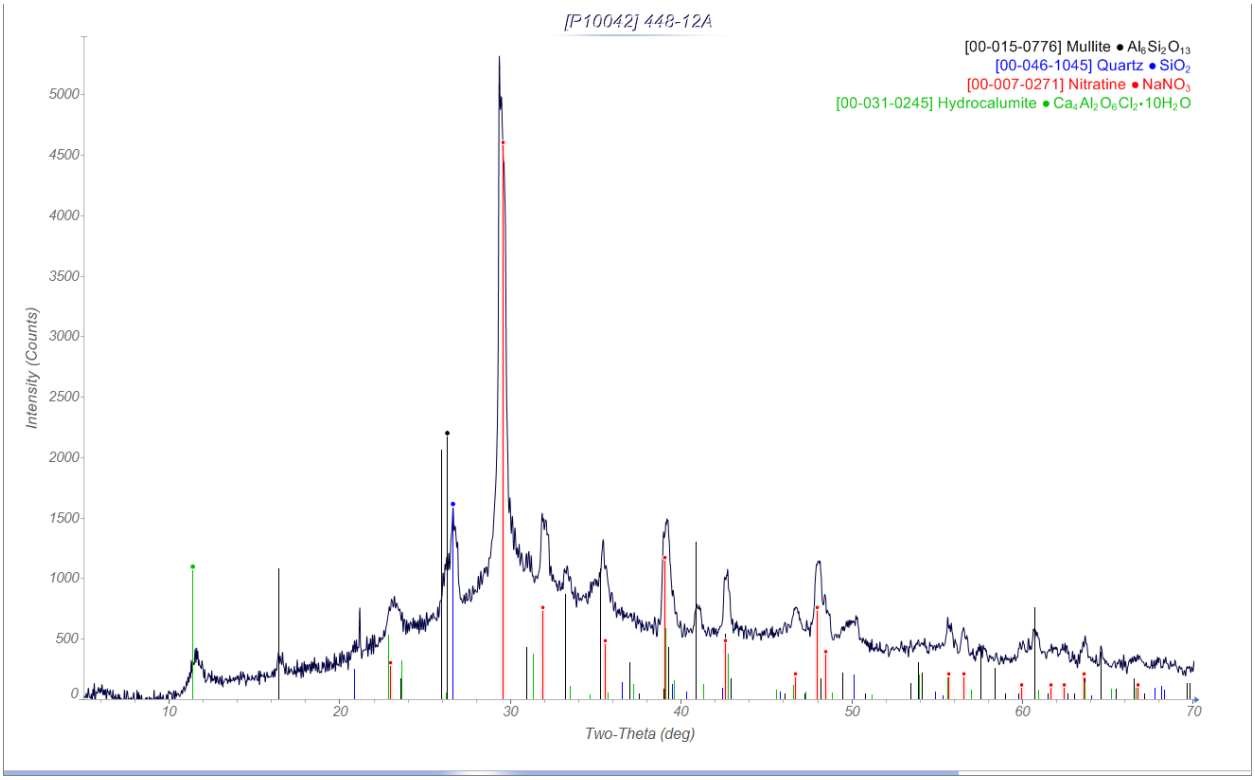
[P10042] 448-12A
[00-015-0776] Mullite • Al6Si2O13
[00-046-1045] Quartz • SiO2
[00-007-0271] Nitratine • NaNO3
[00-031-0245] Hydrocalumite • Ca4Al2O6Cl2·10H2O
Intensity (Counts)
Two-Theta (deg)

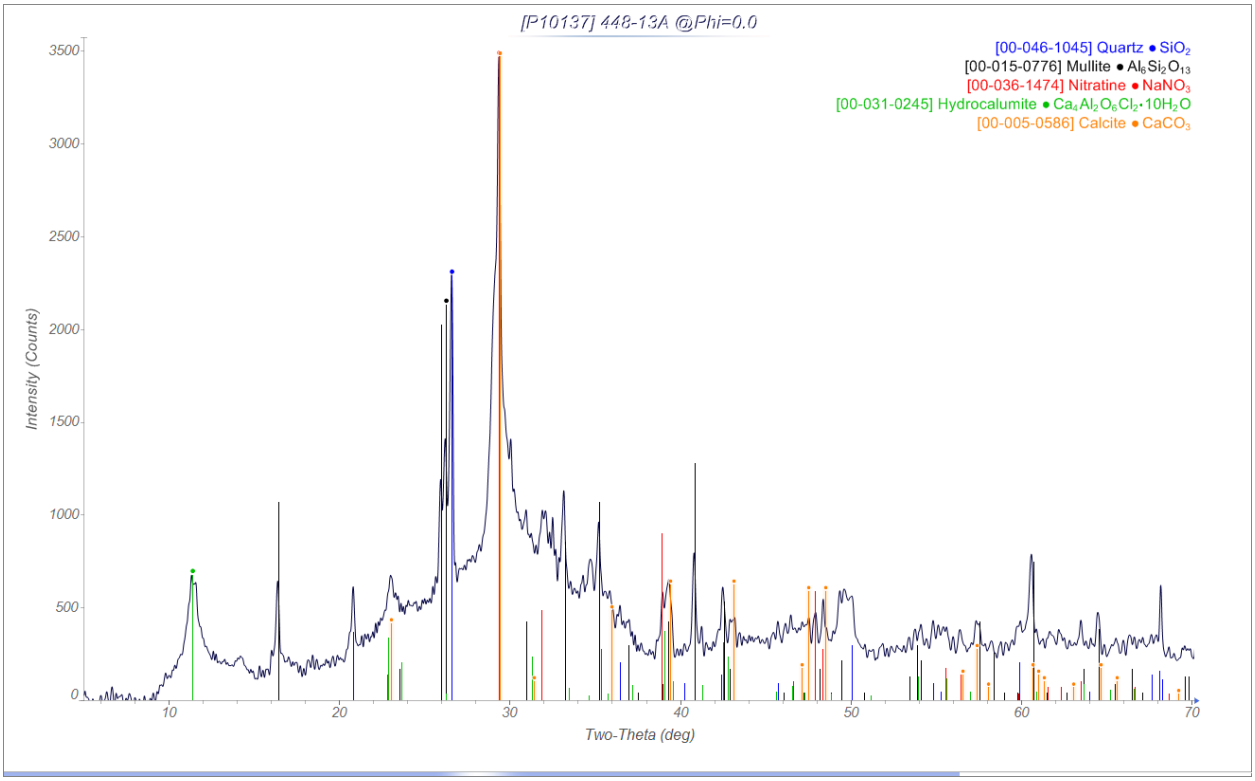
[P10137] 448-13A @Phi=0.0
[00-046-1045] Quartz • SiO2
[00-015-0776] Mullite • Al6Si2O13
[00-036-1474] Nitratine • NaNO3
[00-031-0245] Hydrocalumite • Ca4Al2O6Cl2·10H2O
[00-005-0586] Calcite • CaCO3
Intensity (Counts)
Two-Theta (deg)

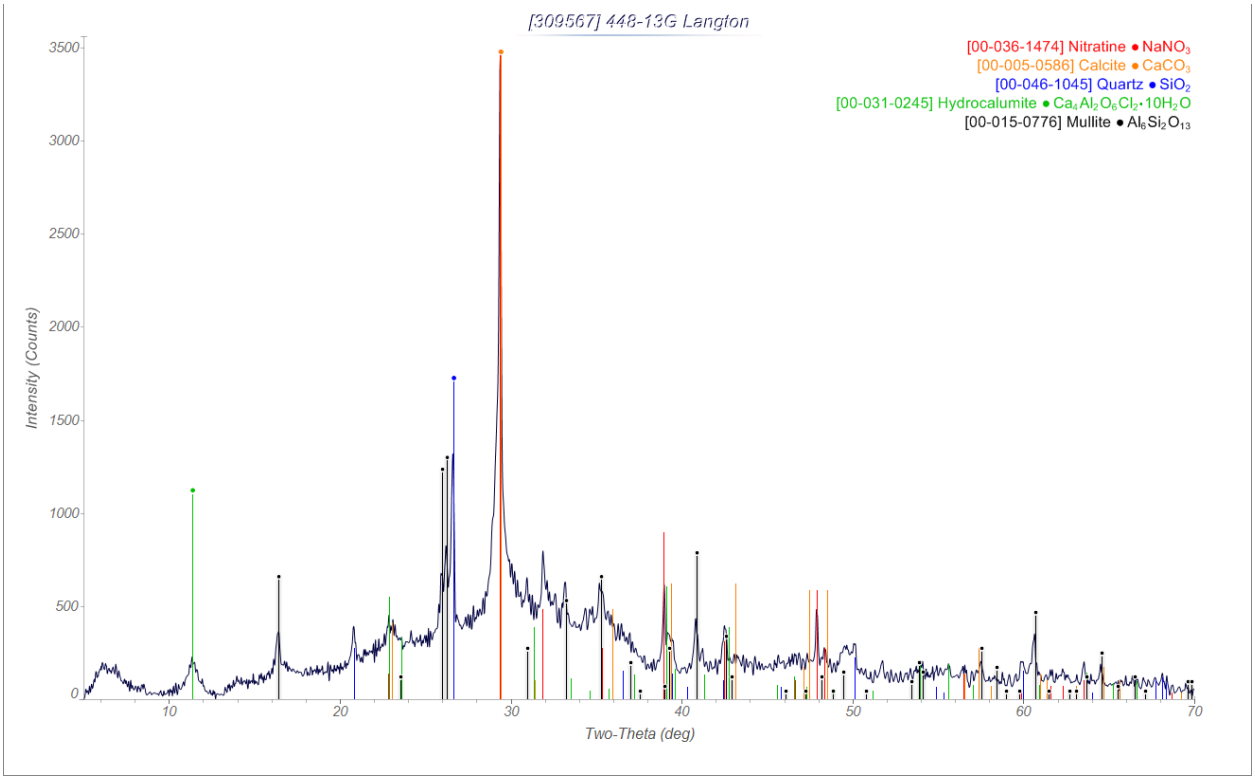
[309567] 448-13G Langton
[00-036-1474] Nitratine • NaNO3
[00-005-0586] Calcite • CaCO3
[00-046-1045] Quartz • SiO2
[00-031-0245] Hydrocalumite • Ca4Al2O6Cl2·10H2O
[00-015-0776] Mullite • Al6Si2O13
Intensity (Counts)
Two-Theta (deg)

Attachment 2. Analysis of Ingredients Used to Prepare Samples

SRNL Process Science Analytical Laboratory
Customer: Alex Cozzi
Date: 3/25/08
Sample ID: 3/08 Cement, 3/08 Slag, 3/08 Fly Ash Lab ID: 08-0630 through 08-0632
Units: wt%
Comments: Li2B4O7 digestion (cations), KOH digestions (anions)

Sample ID	Lab ID													
(wt%)		Al	Ba	Ca	Cr	Fe	K	Mg	Mn	Na	P	S	Si	Ti
3/08 Cement (A)	08-0630	2.78	0.014	46.0	<0.010	2.60	0.511	0.714	0.019	<0.100	0.106	1.16	8.99	0.166
3/08 Cement (B)	08-0630	2.71	0.013	46.0	<0.010	2.75	0.486	0.693	0.019	<0.100	0.103	1.16	9.20	0.162
3/08 Slag (A)	08-0631	4.14	0.030	25.6	<0.010	0.215	0.347	8.00	0.282	0.160	<0.100	0.307	18.6	0.178
3/08 Slag (B)	08-0631	4.29	0.031	26.2	<0.010	0.231	0.356	7.78	0.292	0.174	<0.100	0.303	18.3	0.188
3/08 Fly Ash (A)	08-0632	13.2	0.077	1.76	<0.010	8.96	1.74	0.921	0.012	0.320	0.125	0.159	22.6	0.685
3/08 Fly Ash (B)	08-0632	13.1	0.076	1.74	<0.010	8.95	1.69	0.898	0.011	0.310	0.125	0.150	22.4	0.681

(wt%)		Al2O3	BaO	CaO	Cr2O3	Fe2O3	K2O	MgO	MnO2	Na2O	P2O5	SO4	SiO2	TiO2	Total
3/08 Cement (A)	08-0630	**5.25**	**0.016**	**64.4**	**0.000**	**3.72**	**0.613**	**1.19**	**0.030**	**0.000**	**0.243**	**3.48**	**19.2**	**0.277**	98.5
3/08 Cement (B)	08-0630	**5.12**	**0.015**	**64.4**	**0.000**	**3.93**	**0.583**	**1.15**	**0.030**	**0.000**	**0.236**	**3.48**	**19.7**	**0.271**	98.9
3/08 Slag (A)	08-0631	**7.82**	**0.034**	**35.8**	**0.000**	**0.307**	**0.416**	**13.3**	**0.446**	**0.216**	**0.000**	**0.921**	**39.8**	**0.297**	99.4
3/08 Slag (B)	08-0631	**8.11**	**0.035**	**36.7**	**0.000**	**0.330**	**0.427**	**12.9**	**0.461**	**0.235**	**0.000**	**0.909**	**39.2**	**0.314**	99.6
3/08 Fly Ash (A)	08-0632	**24.9**	**0.086**	**2.46**	**0.000**	**12.8**	**2.09**	**1.53**	**0.019**	**0.432**	**0.286**	**0.477**	**48.4**	**1.14**	94.7
3/08 Fly Ash (B)	08-0632	**24.8**	**0.085**	**2.44**	**0.000**	**12.8**	**2.03**	**1.49**	**0.017**	**0.419**	**0.286**	**0.450**	**47.9**	**1.14**	93.8

		F	Cl	PO4
3/08 Cement (A)	08-0630	<0.200	<0.200	<0.200
3/08 Cement (B)	08-0630	<0.200	<0.200	<0.200
3/08 Slag (A)	08-0631	<0.200	<0.200	<0.200
3/08 Slag (B)	08-0631	<0.200	<0.200	<0.200
3/08 Fly Ash (A)	08-0632	<0.200	<0.200	0.380
3/08 Fly Ash (B)	08-0632	<0.200	<0.200	0.370

						110°C			750°C		LOD (wt%)	LOI (wt%)
Sample ID	Lab ID	Empty (g)	Full (g)	Dry 110°C (g)	Total Solid	Wet Wt (g)	Dry Wt (g)	Dry 750°C (g)	Total Solid			
3/08 Cement (A)	**08-0630**	44.8822	45.8919	45.8897	**99.782%**	1.0097	1.008	45.8814	**98.960%**		**0.200**	**1.05**
3/08 Cement (B)	**08-0630**	44.8358	45.9705	45.9684	**99.815%**	1.1347	1.133	45.9584	**98.934%**			
3/08 Slag (A)	**08-0631**	43.9814	44.9903	44.9902	**99.990%**	1.0089	1.009	44.9901	**99.980%**		**0.057**	**0.134**
3/08 Slag (B)	**08-0631**	43.2951	44.3440	44.3429	**99.895%**	1.0489	1.048	44.3428	**99.886%**			
3/08 Fly Ash (A)	**08-0632**	45.1545	46.1879	46.1863	**99.845%**	1.0334	1.032	46.1408	**95.442%**		**0.125**	**4.54**
3/08 Fly Ash (B)	**08-0632**	44.9127	45.9603	45.9593	**99.905%**	1.0476	1.047	45.9129	**95.475%**			

	Cement A	Cememt B	**Cement Ave**	Slag A	Slag B	**Slag Ave**	Fly Ash A	Fly Ash B	**Fly Ash Ave**
	wt%	wt%	wt%	wt%	wt%	wt%	wt%	wt%	wt%
CaO	64.4	64.4	**64.4**	35.8	36.7	**36.3**	2.4	2.4	**2.4**
MgO	1.19	1.2	**1.2**	13.3	12.9	**13.1**	1.5	1.5	**1.5**
Al2O3	5.25	5.1	**5.2**	7.8	8.1	**8.0**	24.9	24.8	**24.9**
Fe2O3	3.72	3.9	**3.8**	0.3	0.3	**0.3**	12.8	12.8	**12.8**
SiO2	19.2	19.7	**19.5**	39.8	39.2	**39.5**	48.4	47.9	**48.2**
TOTAL	93.76	94.3	94.0	97.0	97.2	97.1	90.1	89.4	89.8

	Normalized Blend	**Normalized Blend**	**Normalized Blend**	**Normalized Blend**	**Normalized Cement**	**Normalized Slag**	**Normalized Class F Fly Ash**
	10:45:45	**25c:75fa**	**25c:75s**	**38s:62fa**			
CaO	24.9	19.2	45.1	15.8	68.5	37.3	2.7
MgO	7.0	1.6	10.4	6.2	1.2	13.5	1.7
Al2O3	16.7	22.2	7.5	20.3	5.5	8.2	27.7
Fe2O3	7.0	11.8	1.3	9.0	4.1	0.3	14.3
SiO2	44.5	45.4	35.7	48.7	20.7	40.7	53.6
Total	100.0	100.0	100.0	100.0	100.0	100.0	100.0
C+M/A+S	0.520	0.307	1.285	0.319	2.66	1.04	0.05
C+M/S+A+F	0.467	0.261	1.248	0.282	2.30	1.03	0.05
C/A+S	0.406	0.284	1.043	0.230	2.61	0.76	0.03


U.S. DEPARTMENT OF
ENERGY


SRNL
SAVANNAH RIVER NATIONAL LABORATORY


CRESP


VANDERBILT
UNIVERSITY


UNITED STATES NUCLEAR REGULATORY COMMISSION


NIST
National Institute of
Standards and Technology


ECN


SIMCO
Technologies inc.

DISTRIBUTION

C. E. Bagwell, 999-W
C. F. Brown, PNNL
T. B. Brown, 773-A
H. H. Burns, 773-41A
P. A. Cavanah, WRPS
A. D. Cozzi, 999-W
D. A. Crowley, 773-43A
J. A. Diediker, DOE-ORP
S. D. Fink, 773-A
G. P. Flach, 773-42A
K. M. Fox, 999-W
J. C. Griffin, 773-A
B. J. Gutierrez, DOE-SR, 704-S
E. K. Hansen, 999-W
C. C. Harrington, DOE-ORP
C. C. Herman, 773-A
E. N. Hoffman, 999-W
V. Jain. 766-H
J. T. Knight, 704-S
C. A. Langton, 773-43A
S. L. Marra, 773-A
F. M. Pennebaker, 773-42A
R. D. Peterson, PNNL
S. H. Pfaff, DOE-ORP
E. M. Pierce, ORNL
W. G. Ramsey, WRPS
K. H. Rosenberger, 705-1C
K. A. Roberts, 773-43A
R. J. Serne, PNNL
S. P. Simner, 249-8H
P. C. Suggs, 704-S
K. H. Subramanian, WRPS
D. J. Swanberg, WRPS
S. A. Thomas, 705-1C
J. H. Westsik, PNNL
W. R. Wilmarth, 773-A